

Polycystin-1 Is a Cardiomyocyte Mechanosensor That Governs L-Type Ca²⁺ Channel Protein Stability

Zully Pedrozo, PhD; Alfredo Criollo, PhD; Pavan K. Battiprolu, PhD; Cyndi R. Morales, PhD; Ariel Contreras-Ferrat, PhD; Carolina Fernández, MSc; Nan Jiang, MSc; Xiang Luo, MD, PhD; Michael J. Caplan, MD, PhD; Stefan Somlo, MD; Beverly A. Rothmel, PhD; Thomas G. Gillette, PhD; Sergio Lavandero, PhD; Joseph A. Hill, MD, PhD

Background—L-type calcium channel activity is critical to afterload-induced hypertrophic growth of the heart. However, the mechanisms governing mechanical stress–induced activation of L-type calcium channel activity are obscure. Polycystin-1 (PC-1) is a G protein–coupled receptor–like protein that functions as a mechanosensor in a variety of cell types and is present in cardiomyocytes.

Methods and Results—We subjected neonatal rat ventricular myocytes to mechanical stretch by exposing them to hypo-osmotic medium or cyclic mechanical stretch, triggering cell growth in a manner dependent on L-type calcium channel activity. RNAi-dependent knockdown of PC-1 blocked this hypertrophy. Overexpression of a C-terminal fragment of PC-1 was sufficient to trigger neonatal rat ventricular myocyte hypertrophy. Exposing neonatal rat ventricular myocytes to hypo-osmotic medium resulted in an increase in α 1C protein levels, a response that was prevented by PC-1 knockdown. MG132, a proteasomal inhibitor, rescued PC-1 knockdown–dependent declines in α 1C protein. To test this in vivo, we engineered mice harboring conditional silencing of PC-1 selectively in cardiomyocytes (PC-1 knockout) and subjected them to mechanical stress in vivo (transverse aortic constriction). At baseline, PC-1 knockout mice manifested decreased cardiac function relative to littermate controls, and α 1C L-type calcium channel protein levels were significantly lower in PC-1 knockout hearts. Whereas control mice manifested robust transverse aortic constriction–induced increases in cardiac mass, PC-1 knockout mice showed no significant growth. Likewise, transverse aortic constriction–elicited increases in hypertrophic markers and interstitial fibrosis were blunted in the knockout animals

Conclusion—PC-1 is a cardiomyocyte mechanosensor that is required for cardiac hypertrophy through a mechanism that involves stabilization of α 1C protein. (*Circulation*. 2015;131:2131–2142. DOI: 10.1161/CIRCULATIONAHA.114.013537.)

Key Words: cardiomegaly ■ mechanotransduction, cellular

Living cells actively sense, integrate, and convert mechanical stimuli into biochemical signals, triggering intracellular responses.¹ In cardiomyocytes, short-term exposure to mechanical stress (MS) results in increased cardiac contractility, whereas long-term stresses are met by structural changes in the myocardium itself.¹ Owing to the limited regenerative potential of cardiomyocytes, cellular hypertrophy, not hyperplasia, is a major mechanism by which these cells cope with increased hemodynamic load.^{1,2} This pathological growth is provoked by abnormal metabolic, structural, and functional events that occur in hypertension, valvular heart disease, myocardial infarction, or mutations in genes coding for contractile proteins.^{1,3} However, mechanisms in cardiomyocytes

underlying the transduction of extracellular mechanical signals into intracellular events (mechanotransduction) are poorly characterized.

Clinical Perspective on p 2142

Polycystin-1 (PC-1) is the protein product of the major gene underlying autosomal-dominant polycystic kidney disease, *Pkd1*.⁴ Eight polycystin genes comprise a novel family of membrane-associated proteins.⁴ Both PC-1 and polycystin-2 (PC-2) are expressed in many different tissues, but their function has been characterized mainly in primary cilia in kidney cells.^{5,6} It is also widely accepted that these proteins act as a complex whereby PC-2 functions as a Ca²⁺ channel and

Received September 29, 2014; accepted April 10, 2015.

From Division of Cardiology, Department of Internal Medicine (Z.P., A.C., P.K.B., C.R.M., N.J., X.L., B.A.R., T.G.G., S.L., J.A.H.) and Department of Molecular Biology (B.A.R., J.A.H.), UT Southwestern Medical Center, Dallas, TX; Advanced Center for Chronic Diseases and Centro de Estudios Moleculares de la Célula, Facultad de Medicina & Facultad de Ciencias Químicas y Farmacéuticas, Santiago, Chile (Z.P., A.C.-F., C.F., S.L.); Instituto de Ciencias Biomédicas, Facultad de Medicina (Z.P., S.L.) and Instituto de Investigación en Ciencias Odontológicas, Facultad de Odontología (A.C.), Universidad de Chile, Santiago; and Departments of Cellular and Molecular Physiology (M.J.C.), Internal Medicine (S.S.), and Genetics (S.S.), Yale University School of Medicine, New Haven, CT.

The online-only Data Supplement is available with this article at <http://circ.ahajournals.org/lookup/suppl/doi:10.1161/CIRCULATIONAHA.114.013537/-/DC1>.

Correspondence to Joseph A. Hill, MD, PhD, Cardiology Division, Department of Internal Medicine, UT Southwestern Medical Center, 6000 Harry Hines Blvd, Dallas, TX 75390–8573. E-mail joseph.hill@utsouthwestern.edu; or Sergio Lavandero, PhD, Advanced Center for Chronic Diseases (ACCDiS), Facultad de Ciencias Químicas & Facultad de Medicina, Universidad de Chile, Olivos 1007, Santiago 8380492, Chile. E-mail slavander@uchile.cl

© 2015 American Heart Association, Inc.

Circulation is available at <http://circ.ahajournals.org>

DOI: 10.1161/CIRCULATIONAHA.114.013537

PC-1 is a sensor of shear stress. However, PC-1 and PC-2 can operate independently.^{7,8} In fact, PC-1 can act as a mechanosensor independently of shear stress.^{9–11}

L-type Ca²⁺ channel (LTCC) activity plays a key role in the cardiomyocyte response to MS.¹² Yet, how MS regulates LTCC function and which mechanosensor(s) are involved in the heart are unclear.

The mechanisms of mechanotransduction in heart are poorly understood. Furthermore, in cardiomyocytes, it is unknown what role, if any, PC-1 plays in physiological and pathological events. That being said, PC-1 has been implicated in pathways central to the development of cardiac hypertrophy such as mammalian target of rapamycin and calcineurin/nuclear factor of activated T cells.¹³ Therefore, we set out to explore a possible role for PC-1 in the development of pressure overload–induced cardiac hypertrophy.

Methods

All studies conform to the *Guide for the Care and Use of Laboratory Animals* published by the US National Institutes of Health (8th Edition, 2011) and were approved by the Institutional Ethics Review Committees of the University of Texas Southwestern Medical Center and Universidad de Chile.

Cardiomyocyte Culture and Transfections

Neonatal rat ventricular myocytes (NRVMs) were isolated from the ventricles of Sprague-Dawley rat pups on postnatal day 1 to 2. Cells were preplated to enrich for cardiomyocytes, plated, and cultured for 24 hours in Dulbecco modified Eagle medium/M199 (3:1) containing 5% FBS, 10% horse serum, and 100 μmol/L BrdU (Sigma-Aldrich).¹⁴ For PC-1 knockdown, NRVMs were transfected overnight with 2 sequence-independent siRNAs specific for PC-1 (120 nmol/L, Sigma-Aldrich) with oligofectamine (Invitrogen). Decreases in PC-1 mRNA and protein were optimized in terms of both concentration (60–200 nmol/L) and time (6, 12, 24, and 48 hours). Stimuli were applied 24 hours after transfection. For lentivirus-mediated overexpression of PC-1 C-terminal peptide, cells were infected at a multiplicity of infection of 15 plaque-forming units per cell and subsequently harvested in Trizol or T-PER buffer (Thermo Scientific) containing phosphatase and protease inhibitors (Roche) for harvesting mRNA or protein, respectively.

PC-1 Knockout Mice

Male mice harboring a cre recombinase transgene driven by an α-myosin heavy chain (α-MHC) promoter were crossed with mice harboring floxed *Pkd-1* alleles¹⁵ to generate PC-1 knockout (PC-1 KO) mice. Mendelian frequencies in the birthrate were normal. Genotyping was performed by polymerase chain reaction (PCR). Primers used for PCR are listed in Table I in the online-only Data Supplement. PC-1 silencing was confirmed by Western blot and reverse transcription–PCR for *Pkd-1* mRNA in cardiac tissue. *Pkd-2* (gene encoding PC-2) mRNA levels were also evaluated in these animals. Nine- to 11-week-old mice were used in this study. Both α-MHC–cre and F/F mice were used as controls.

Model of Pressure Overload

Male α-MHC–cre and PC-1 KO mice (9–11 weeks old) were subjected to pressure overload by surgical transverse aortic constriction (TAC).¹⁶ After 3 weeks, animals were euthanized, and proteins and mRNA were harvested.

[³H]Leucine Incorporation

Cultured NRVMs were stimulated and incubated with [³H]Leucine (1 mCi/mL; Perkin-Elmer). After treatment, NRVMs were washed

3 times with ice-cold PBS and incubated with 10% trichloroacetic acid (30 minutes at 4°C), followed by 3 washes with ice-cold 95% ethanol. Cells were then lysed in 1 mL 0.5 mol/L NaOH (6 hours at 37°C) with gentle agitation. Lysates were neutralized with 1 mL 0.5 mol/L HCl, and the total content from each well was processed by scintillation counting (Beckman).

Histology

All tissues were fixed in 4% paraformaldehyde and transferred to 1× PBS, followed by paraffin embedding. Hematoxylin/eosin staining was performed for morphological analyses. Wheat germ agglutinin was used for cross-sectional area measurements, quantified from at least 25 cells per section and 2 sections per group. Masson trichrome staining was used for measurements of fibrosis and quantified with ImageJ software.

RNA Isolation and Quantitative Reverse Transcription–PCR

Total RNA was isolated from mouse tissues or NRVMs with an Aurum total RNA Mini Kit according to the recommendations of the manufacturer (Bio-Rad). RNA (150 ng) from each sample was used for reverse transcription using the iScript cDNA synthesis kit (Bio-Rad). cDNA was diluted 10-fold with ddH₂O and used for quantitative PCR analysis (Roche). Primers used for reverse transcription–PCR are listed in Table II in the online-only Data Supplement. A ΔCt method was used to calculate relative transcript abundances.

Western Blot

Proteins from mouse tissue or NRVMs were separated by SDS-PAGE, transferred to a supported nitrocellulose membrane, and immunoblotted. PC-1, LTCC subunit (α1C, β2, α2δ), and GAPDH antibodies were purchased from Santa Cruz Biotechnology. Other antibodies used include RCAN (Sigma), β-myosin heavy chain (β-MHC), and PC-1 (Abcam), and ERK (Cell Signaling). Blots were scanned and quantified with an Odyssey Licor (version 3.0) imaging system. Results were normalized to GAPDH.

Echocardiography

Echocardiograms were performed on conscious, gently restrained mice with either a Sonos 5500 system with a 15-MHz linear probe or a Vevo 2100 system with a MS400C scan head. Left ventricular (LV) end-diastolic dimension (LVEDD) and LV end-systolic dimension (LVESD) were measured from M-mode recordings. Fractional shortening was calculated as (LVEDD–LVESD)/LVEDD and expressed as a percentage. LV mass was calculated by the cubed method as 1.05×[(IVS+LVID+LVPW)³–LVID³], where IVS is interventricular septum thickness, LVID is LV internal diameter, and LVPW is LV posterior wall thickness, and expressed in milligrams.¹⁴ All measurements were made at the level of the papillary muscles.

Protein Biotinylation

Plasma membrane proteins from NRVMs were isolated with the use of a biotinylation kit according to the recommendations of the manufacturer (Thermo Scientific). We loaded equivalent protein amounts and separated them by SDS-PAGE, and membranes were blotted with α1C LTCC antibody.

Coimmunoprecipitation

NRVMs were collected and lysed with buffer lysis containing Tris-HCl, pH 7 (50 mmol/L), NaCl (120 mmol/L), Nonidet P-40 (0.5%), and a protease inhibitor cocktail (Complete, Roche Diagnostic). The lysate was centrifuged (4°C at 10 minutes and 10000g), and the supernatant was collected and immunoprecipitated with anti-α1C or anti-β2 LTCC and protein A/G-Sepharose (Sigma-Aldrich). The immunoprecipitates were analyzed by Western blot with anti-α1C or anti-β2 antibodies.

Cyclic Mechanical Stretch

NRVMs were cultured on flexible membrane plates coated with collagen IV for adherence (Flexcell Bioflex plates). After 24 hours of culture, the cells were serum starved for 24 hours. For mechanical stretch, we used a computer-regulated vacuum strain apparatus (Flexcell Strain Unit FX-4000 Tension Plus, Flexcell International), and cycles of stretch and relaxation were applied (1 Hz, 20% stretch, 2 hours). Control cells were maintained under static conditions.

Duolink Assay

Duolink staining (Sigma) was performed according to the manufacturer's guidelines and previous reports.¹⁷ For PC-1/ α 1C interaction, we used either mouse anti-PC-1 (Abcam) and rabbit anti- α 1C (Santa Cruz Biotechnology) or rabbit anti-PC-1 (Santa Cruz Biotechnology) and mouse anti- α 1C primary antibodies. Images were obtained via confocal microscopy.

Other Procedures

Lactate dehydrogenase activity was measured in the supernatant of NRVM cultures with a CytoTox 96 Non-Radioactive Cytotoxicity Assay according to the recommendations of the manufacturer (Promega). Proteins were quantified according to the Bradford method.

Reagents

After 24 hours of serum starvation, NRVMs were exposed to hypo-osmotic stress (HS) by exposure to medium diluted 1:1 with double-distilled H₂O. The osmolality of the Dulbecco modified Eagle medium/M199 diminished from 250 to 125 mOsmol/kg. Phenylephrine was used at 50 μ mol/L. All inhibitors were added 30 minutes before the corresponding stimulus or measurement: nifedipine (10 μ mol/L), verapamil (10 μ mol/L), cycloheximide (35 μ mol/L), gadolinium chloride (10 μ mol/L), MG132 (1 μ mol/L), SKF 96365 (10 μ mol/L), and trolox (100 μ mol/L).

Statistical Analysis

Data are presented as mean \pm SEM of multiple independent replicates. Data were analyzed either by the Student unpaired *t* test to compare means when there were 2 experimental groups or by the Welch version of 1-way ANOVA followed by the Tukey test to compare means among ≥ 3 groups. Data were analyzed statistically with IBM SPSS Statistics software, version 21. Differences were considered significant at *P*<0.05.

Results

PC-1 Mediates Cardiomyocyte Hypertrophy Induced by Mechanical Stretch In Vitro

PC-1 has been proposed to act as a mechanosensor in a variety of cell types, regulating cell growth and differentiation.⁸ Furthermore, PC-1 activity has been shown to trigger activation of the calcineurin/nuclear factor of activated T cells (NFAT) pathway in both T cells and osteoblasts.^{13,18} Because the calcineurin/NFAT pathway is central to the development of pressure overload–induced hypertrophy,¹⁹ we set out to test for a possible role of PC-1 in stretch-induced cardiomyocyte growth responses. To initially examine this, we knocked down PC-1 in NRVMs using targeted siRNA (Figure 1A and 1B in the online-only Data Supplement) and induced hypertrophy using an in vitro model of mechanical stretch by exposure to HS medium.²⁰ These results were compared with cells exposed to nonsense siRNA and with cells in which hypertrophy was induced neurohumorally with phenylephrine. Hypertrophic growth was assayed as [³H]Leucine incorporation.

Both phenylephrine and HS triggered an increase in [³H]Leucine incorporation after 48 hours in cells transfected with control siRNA (Figure 1A). PC-1–specific siRNA treatment

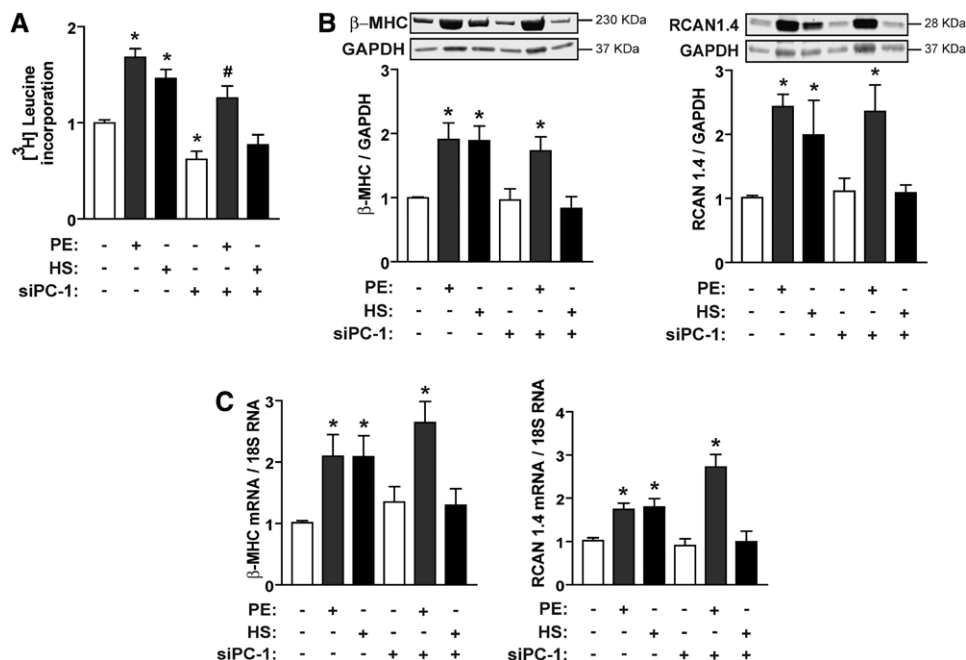


Figure 1. Polycystin-1 (PC-1) mediates in vitro cardiomyocyte hypertrophy. **A**, [³H]Leucine incorporation in cardiomyocytes stimulated with phenylephrine (PE) or hypo-osmotic stress (HS) and exposed to PC-1 siRNA (siPC-1) or transfected with unrelated sequences. **B**, Representative Western blot of β -myosin heavy chain (β -MHC; left) and RCAN1.4 (right). Mean data of β -MHC/GAPDH and RCAN1.4/GAPDH calculated from densitometric analysis after hypertrophic stimuli. **C**, mRNA levels of β -MHC and RCAN1.4 are depicted as β -MHC/18S (left) and RCAN1.4/18S (right), respectively. Values are mean \pm SEM, analyzed by the Welch test of 1-way ANOVA followed by the Tukey test (*n*=5–8). **P*<0.05 vs control; #*P*<0.05 vs siPC-1.

had no effect on the ability of phenylephrine to induce hypertrophy but elicited a marked inhibition of HS-induced hypertrophy. Importantly, this growth-suppression effect was observed with the use of a second, sequence-independent siRNA construct targeting PC-1 (data not shown).

We next tested for a requirement of PC-1 in the induction of markers of hypertrophy. Consistent with the protein synthesis assay, phenylephrine treatment resulted in an increase in hypertrophic markers, including an increase in both β -MHC and RCAN1.4 protein levels (Figure 1B) and mRNA levels (Figure 1C), even in the absence of PC-1. In contrast, PC-1 knockdown significantly attenuated HS-induced increases in both β -MHC and RCAN1.4 levels (Figure 1B and 1C). Importantly, HS treatment did not result in significant cell death during the 48-hour treatment period compared with control (Figure 1C in the online-only Data Supplement). Together, these data suggest that PC-1 is required for cardiomyocyte growth triggered by HS-induced stretch but not phenylephrine-induced cell growth. Additionally, they suggest involvement of PC-1 in activating the calcineurin/NFAT signaling cascade.

The calcineurin/NFAT and extracellular signal-regulated kinase (ERK) 1/2 signaling cascades are involved in hypertrophic growth in cardiomyocytes and appear to be interdependent.²¹ During mechanical stretch, ERK1/2 is activated early after stimulus onset.²⁰ In our model, HS treatment also resulted in an early increase in ERK1/2 phosphorylation within 1 to 2 hours after stimulus onset, which decreased back to baseline at 4 to 8 hours (Figure 1D in the online-only Data Supplement). Knockdown of PC-1 suppressed this increase

in ERK1/2 phosphorylation, suggesting that PC-1 may also modulate ERK1/2 activation. Together, these data are consistent with a model in which PC-1 acts as a mechanosensor in cardiomyocytes and mediates hypertrophy induced by mechanical stretch.

L-Type Calcium Channel Is Involved in Mechanical Stretch–Induced Cardiomyocyte Hypertrophy

One of the crucial triggers of cardiac hypertrophy is a sustained increase in cytoplasmic Ca^{2+} .²² These increases in cytoplasmic Ca^{2+} arise, at least in part, from increased Ca^{2+} influx via LTCC activity and store-operated calcium entry (SOCE).^{12,23,24} Given this, we tested the role of LTCC in HS-induced cardiomyocyte hypertrophy. NRVMs were exposed to HS in the presence or absence of LTCC inhibitors, and hypertrophy was measured as [³H]Leucine incorporation. Exposure of NRVMs to 2 structurally distinct LTCC inhibitors (verapamil, nifedipine; 10 μ mol/L) completely inhibited HS-induced increases in [³H]Leucine incorporation, confirming a role for LTCC in this response (Figure 2A).²⁵ Interestingly, Gd^{3+} , which inhibits SOCE and a number of other channels, did not suppress [³H]Leucine incorporation in NRVMs after HS stimulation (Figure 2B), suggesting that SOCE-induced increases in Ca^{2+} are not involved in HS-induced hypertrophy.

The requirement for LTCC activity in HS-induced hypertrophy was confirmed by measuring molecular markers of hypertrophy. HS-induced activation of both β -MHC and RCAN1.4 mRNA levels was inhibited by LTCC inhibitors (Figure 2C). These data demonstrate a requirement for

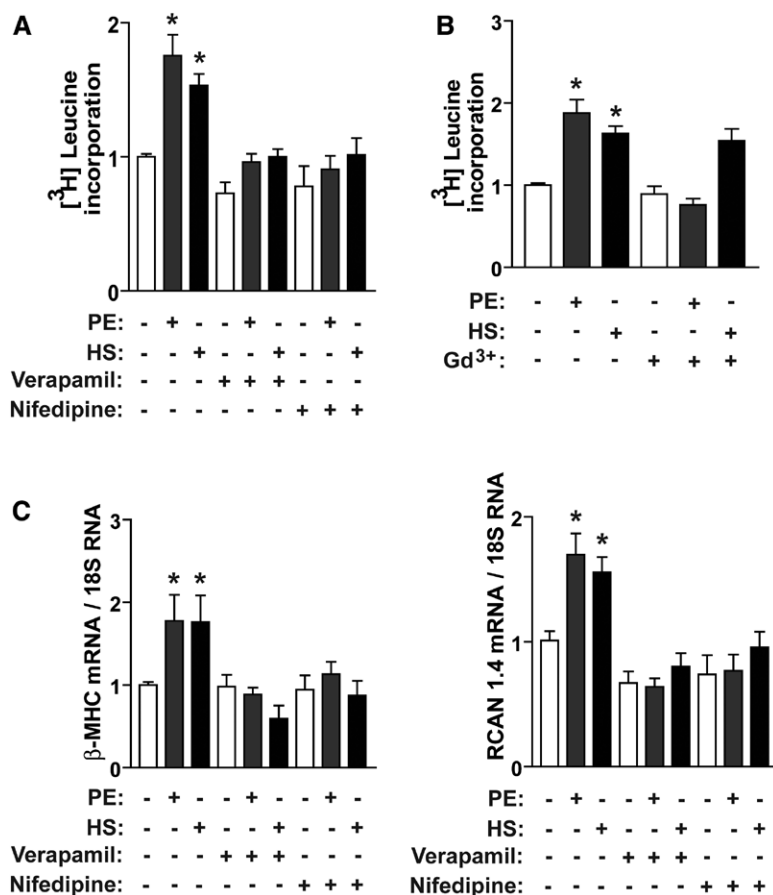


Figure 2. L-type calcium channel activity is required for mechanical stretch–induced cardiomyocyte hypertrophy. **A** and **B**, [³H]Leucine incorporation in cardiomyocytes stimulated with phenylephrine (PE) or hypo-osmotic stress (HS) in the presence of verapamil, nifedipine, or Gd^{3+} . **C**, Ratios of β -myosin heavy chain (β -MHC)/18S (left) and RCAN1.4/18S (right) transcripts. Values are mean \pm SEM analyzed by the Welch test of 1-way ANOVA followed by the Tukey test ($n=4-6$). * $P<0.05$ vs control.

LTCC activity in HS-induced hypertrophy. Furthermore, the inability of Gd^{3+} to inhibit HS-induced hypertrophy is interesting in light of our earlier report that hypertrophy induced by neurohumoral cues (phenylephrine) is inhibited by Gd^{3+} (Figure 2B).²⁴ Together, these data support a model in which LTCC is required to induce cardiomyocyte hypertrophy by mechanical stretch, suggesting that PC-1 modulates this pathway. They also demonstrate that HS-induced hypertrophy requires both functional LTCC activity and PC-1.

PC-1 Promotes LTCC Stabilization During HS Stress

Ca^{2+} influx through the LTCC is regulated a number of ways.²⁶ Among these regulatory mechanisms, governance of channel density in the plasma membrane is prominent.²⁶⁻²⁸ To

determine whether LTCC protein abundance is altered after HS treatment, we measured steady-state levels of LTCC protein by Western blot. Interestingly, 1 hour of exposure to HS triggered >2-fold increases in $\alpha 1C$ protein, a change that was maintained at least after 4 hours of HS exposure (Figure 3A). Knockdown of PC-1 resulted in a decrease in steady-state $\alpha 1C$ levels at baseline (Figure 3A), lasting for at least 48 hours (Figure 3B). Furthermore, PC-1 silencing blunted HS-induced increases in $\alpha 1C$ protein levels (Figure 3A). These data demonstrate that HS-induced increases in $\alpha 1C$ protein are dependent on PC-1 and suggest a mechanism whereby PC-1 may regulate MS-induced hypertrophy.

Whereas steady-state levels of $\alpha 1C$ protein were increased by HS treatment, increased LTCC activity, and consequent

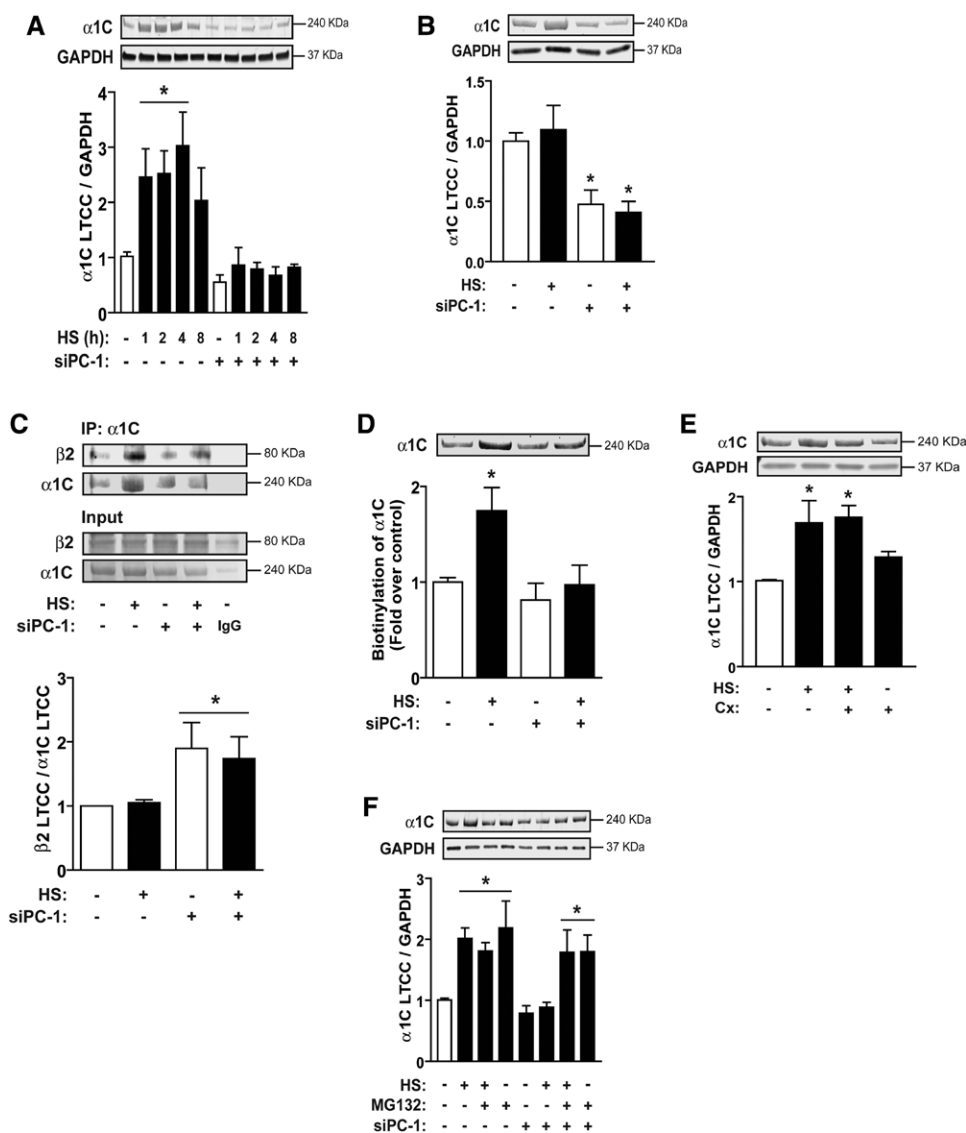


Figure 3. Polycystin-1 (PC-1) stabilizes the $\alpha 1C$ L-type calcium channel (LTCC) subunit protein. **A**, Time course of changes in $\alpha 1C$ /GAPDH ratios from Western blot densitometric analysis. **B**, Representative Western blot for $\alpha 1C$ and GAPDH and for $\alpha 1C$ /GAPDH ratio in cardiomyocytes stimulated with hypo-osmotic stress (HS; 48 hours) in the setting of PC-1 knockdown (siPC-1). **C**, Immunoprecipitation of the $\alpha 1C$ subunit and Western blot for the $\beta 2$ and $\alpha 1C$ subunits from siPC-1 and control cells stimulated with HS and their densitometric quantification. **D**, Plasmalemmal surface protein biotinylated after HS stimulation (2 hours) in siPC-1 and control cells. Representative Western blots and densitometric analysis for $\alpha 1C$. **E**, $\alpha 1C$ /GAPDH ratios from immunoblot analysis of cells stimulated with HS (2 hours) in the presence of cycloheximide (Cx). **F**, $\alpha 1C$ and GAPDH protein levels by Western blot, as well as quantified ratios of $\alpha 1C$ /GAPDH, from siPC-1 and control cardiomyocytes stimulated with HS (2 hours) in the presence or absence of MG132. Values are mean \pm SEM analyzed by the Welch test of 1-way ANOVA followed by the Tukey test (n=3-5). * P <0.05 vs control.

Ca²⁺ influx, requires localization of LTCC to the plasma membrane, a process regulated by the β 2 subunit.²⁹ To test for β 2 subunit involvement, we performed immunoprecipitation assays to determine whether increases in α 1C protein correlated with an increase in β 2 subunit interaction. Exposure of NRVMs to HS for 2 hours resulted in an increase in the amount of β 2 subunit harvested with an α 1C antibody, a change that is roughly proportional to increases in α 1C levels (Figure 3C). Importantly, those increases were absent in cells depleted of PC-1 (Figure 3C). The steady-state levels of the α 2 δ did not change in NRVMs depleted of PC-1 or stimulated with HS (Figure IE in the online-only Data Supplement). These data then are consistent with a model in which increases in α 1C protein contribute to HS-induced cardiomyocyte hypertrophy and point to PC-1 as an upstream regulator.

To quantify LTCC abundance on the cardiomyocyte cell surface more directly, we selectively biotinylated surface proteins under conditions of HS stress. We isolated biotinylated proteins and analyzed equivalent amounts of protein by SDS-PAGE. In control cells, HS treatment resulted in an increase in plasma membrane-associated α 1C, but that increase was absent in PC-1 knockdown cells (Figure 3D). These findings suggest that PC-1 is required for MS-induced increases in LTCC at the cell surface.

Increases in steady-state levels of α 1C could result from increased expression or decreased turnover of the protein. To assess the role of protein expression, we measured the change in steady-state levels of α 1C after HS (2 hours) in the presence of the protein translation inhibitor cycloheximide (35 μ mol/L) 20 minutes before and during the HS stimulus. Inhibition of new protein synthesis had no impact on HS-induced increases in α 1C protein (Figure 3E), suggesting that α 1C protein degradation is a major mechanism of PC-1-dependent control.

Plasma membrane levels of LTCC are regulated in part by proteasomal degradation of α 1C subunit.²⁹ To assess the role of the ubiquitin-proteasome system in HS-induced increases in α 1C subunit protein, we treated NRVMs with the proteasome inhibitor MG132 (1 μ mol/L). Exposure to MG132 (2 hours) provoked increases in α 1C levels similar to those observed in HS-treated cells. Importantly, adding MG132 to HS-treated cells did not further increase α 1C levels. In addition, MG132 treatment restored α 1C levels in cells silenced for PC-1 (Figure 3F). These data suggest that declines in α 1C in HS-treated cells subjected to PC-1 knockdown derive from increased proteasomal turnover. Furthermore, they suggest that increases in LTCC levels triggered by HS-induced MS are driven by decreased proteasomal turnover.

Having uncovered PC-1-dependent stabilization of LTCC in response to HS, we next examined a different model of MS elicited by cyclic mechanical stretch.²⁰ Exposure of NRVMs to MS for 2 hours resulted in induction of the calcineurin/NFAT pathway, as evidenced by increases in RCAN1.4 protein levels (Figure IF in the online-only Data Supplement) and ERK1/2 activation (Figure IG in the online-only Data Supplement). siRNA knockdown of PC-1 inhibited the induction of these signaling pathways by MS. Importantly, steady-state levels of α 1C manifested stretch-induced increases in a manner dependent on the presence of PC-1 (Figure IH in the online-only Data Supplement). Additionally, SKF 96365 (10 μ mol/L), a

specific SOCE inhibitor, did not prevent the increase in α 1C protein levels or RCAN1.4 after MS stimulation (Figure II and IJ in the online-only Data Supplement), in agreement with our observation that SOCE is not involved in stretch-induced hypertrophy. Not surprisingly, although nifedipine, an LTCC inhibitor, blocked MS-induced stimulation of RCAN1.4, it did not affect MS-induced increases in α 1C (Figure II and IJ in the online-only Data Supplement). Together, these data confirm our findings with HS-induced mechanical stretch and lend further support to a model of PC-1-dependent mechanosensation and LTCC protein stabilization in the development of hypertrophy.

MS-induced reactive oxygen species (ROS) accumulation triggers increases in Ca²⁺ spark frequency.³⁰ Given this, we tested whether ROS are involved in LTCC stabilization. Depleting ROS with the scavenger compound trolox, however, had no effect, suggesting that ROS accumulation is not a major mechanism governing stabilization of LTCC by PC-1 (Figure IK in the online-only Data Supplement).

PC-1 C Terminus Is Sufficient to Promote LTCC Stabilization and Cardiomyocyte Hypertrophy

The \approx 200-aa, cytoplasmic C-terminal tail of PC-1 has been implicated in a number of downstream signaling events; furthermore, it can be cleaved and localized to the nucleus via a nuclear localization signal present within its sequence.³¹ To test for a potential role in the development of cardiac hypertrophy, we infected cells with lentivirus expressing the C-terminal tail (p200; Figure IL in the online-only Data Supplement).³² Overexpression of p200 in NRVMs resulted in a nearly 2-fold increase in [³H]Leucine incorporation compared with control-infected cells (Figure 4A). This cardiomyocyte growth was abolished by treatment with nifedipine (Figure 4A). The p200-induced increase in [³H]Leucine incorporation was also associated with an increase in β -MHC and RCAN1.4 protein and RCAN1.4 mRNA levels, markers of cardiac hypertrophy (Figure 4B).

Our earlier data suggested that the PC-1-dependent effects on hypertrophy were independent of the ability of PC-1 to activate a transcriptional response (Figure 3E). This would suggest that the ability of p200 to induce hypertrophy is independent of p200 nuclear localization. To test this, we engineered a lentivirus harboring p200 protein lacking the nuclear localization signal (p200 Δ). Expression of p200 Δ triggered increases in [³H]Leucine incorporation similar to those observed with p200 (Figure 4A and Figure IL in the online-only Data Supplement).

Our findings reveal that PC-1 is required for a stretch-induced hypertrophic response in NRVMs in a manner that requires both LTCC function and increases in LTCC surface localization. Furthermore, overexpression of the C-terminal domain of PC-1 was sufficient to recapitulate the effects of full-length PC-1. To examine whether the p200-induced hypertrophic response results in an increase of LTCC biosynthesis, we performed both Western analysis and immunoprecipitation experiments. As observed with HS treatment, protein, but not mRNA, levels of α 1C were significantly increased after 48 hours of p200 expression (Figure 4C). Furthermore, increased association of α 1C and β 2 LTCC subunits was observed in

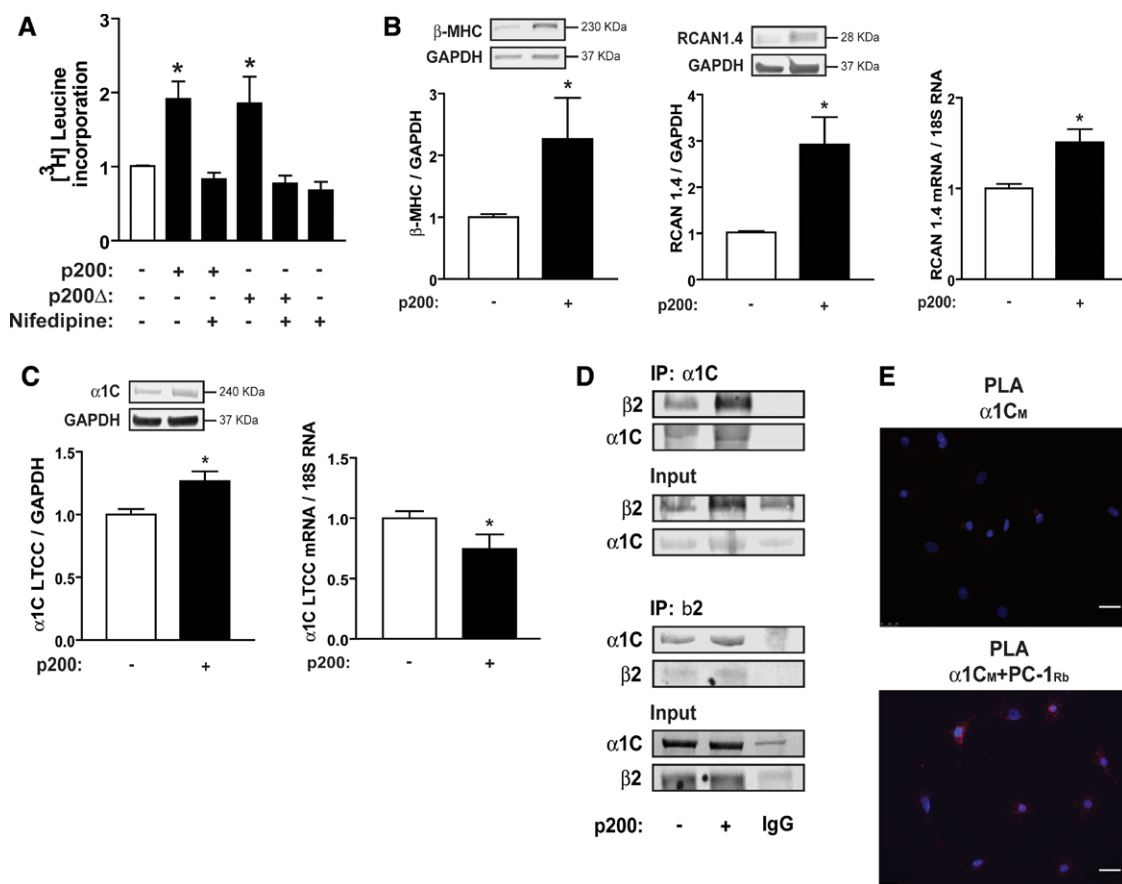


Figure 4. Overexpression of polycystin-1 (PC-1) C terminus induces cardiomyocyte hypertrophy. **A**, [³H]Leucine incorporation in cardiomyocytes transfected with a C-terminal PC-1 peptide (p200) or the C terminus lacking the nuclear localization signal (p200Δ). Nifedipine was used as the L-type calcium channel (LTCC) blocker. **B**, Representative Western blots of β-myosin heavy chain (β-MHC; left) and RCAN1.4 (middle) and RCAN1.4 mRNA (right) in cardiomyocytes transfected (48 hours) with p200, as well as quantified data of β-MHC/GAPDH, RCAN1.4/GAPDH, and RCAN1.4/18S. **C**, Left, Quantification of protein levels and representative Western blot of the α1C subunit in cells transfected with p200 (48 hours). Right, α1C mRNA levels depicted as an α1C/18S ratio in identical experiments. **D**, Immunoprecipitation of α1C and β2 subunit from cardiomyocytes transfected with p200. Representative Western blots of α1C and β2 are shown for each of the immunoprecipitations. **E**, Representative image of neonatal rat ventricular myocytes fixed and probed with anti-α1C antibody (mouse [M]) and anti-PC-1 antibody (rabbit [Rb]) for proximity ligation assay (PLA). Top, Control using only the α1C primary antibody (not the PC-1 antibody) followed by both secondary antibodies. Bottom, Cells were incubated with both PC-1 and α1C primary antibodies, resulting in the formation of distinct puncta, indicating that the 2 secondary antibodies are in close proximity. Values are mean±SEM analyzed by the Student unpaired *t* test or Welch test of 1-way ANOVA followed by the Tukey test (*n*=4–6). **P*<0.05 vs control.

reciprocal immunoprecipitation assays (Figure 4D). These data are consistent with a model in which the C terminus of PC-1 acts to trigger hypertrophic growth in response to MS.

PC-1 Interacts With LTCC

Having confirmed a functional link between PC-1 and α1C, we next tested for evidence of a physical interaction between the proteins. Because standard immunoprecipitation experiments with membrane channel proteins can be problematic, we used a proximity ligation assay to test for regulated physical proximity between PC-1 and α1C. NRVMs grown on coverslips were fixed and incubated with primary antibodies targeting α1C (mouse antibody) and PC-1 (rabbit antibody). Cells were next exposed to corresponding DNA-linked secondary antibodies, and the slides were processed according to the manufacturer’s instructions (Duolink, Sigma). Probing the cells with only the mouse α1C primary antibody (and not the PC-1 antibody) resulted in minimal background signal.

In contrast, probing with both rabbit PC-1 and mouse α1C primary antibodies resulted in the formation of numerous distinct puncta, indicating that the 2 secondary antibodies are in close proximity (<40 nm; Figure 4E). Similar results were obtained independently with a rabbit α1C primary antibody and mouse PC-1 primary antibody (Figure IM in the online-only Data Supplement). These findings then suggest that PC-1 and LTCC proteins interact physically under basal conditions.

PC-1 Is Required for Cardiac Hypertrophy and Normal Heart Function

To define the role of PC-1 in adult heart, we engineered a line of mice with cardiomyocyte-restricted silencing of PC-1 (α-MHC-cre; *Pkd1*^{fl/fl}; henceforth referred to as PC-1 KO). Recombination in these hearts was confirmed by PCR, and Western blot analysis of protein extracts from these hearts confirmed cardiomyocyte-specific loss of PC-1 (Figure 5A and Figure IIA in the online-only Data Supplement).

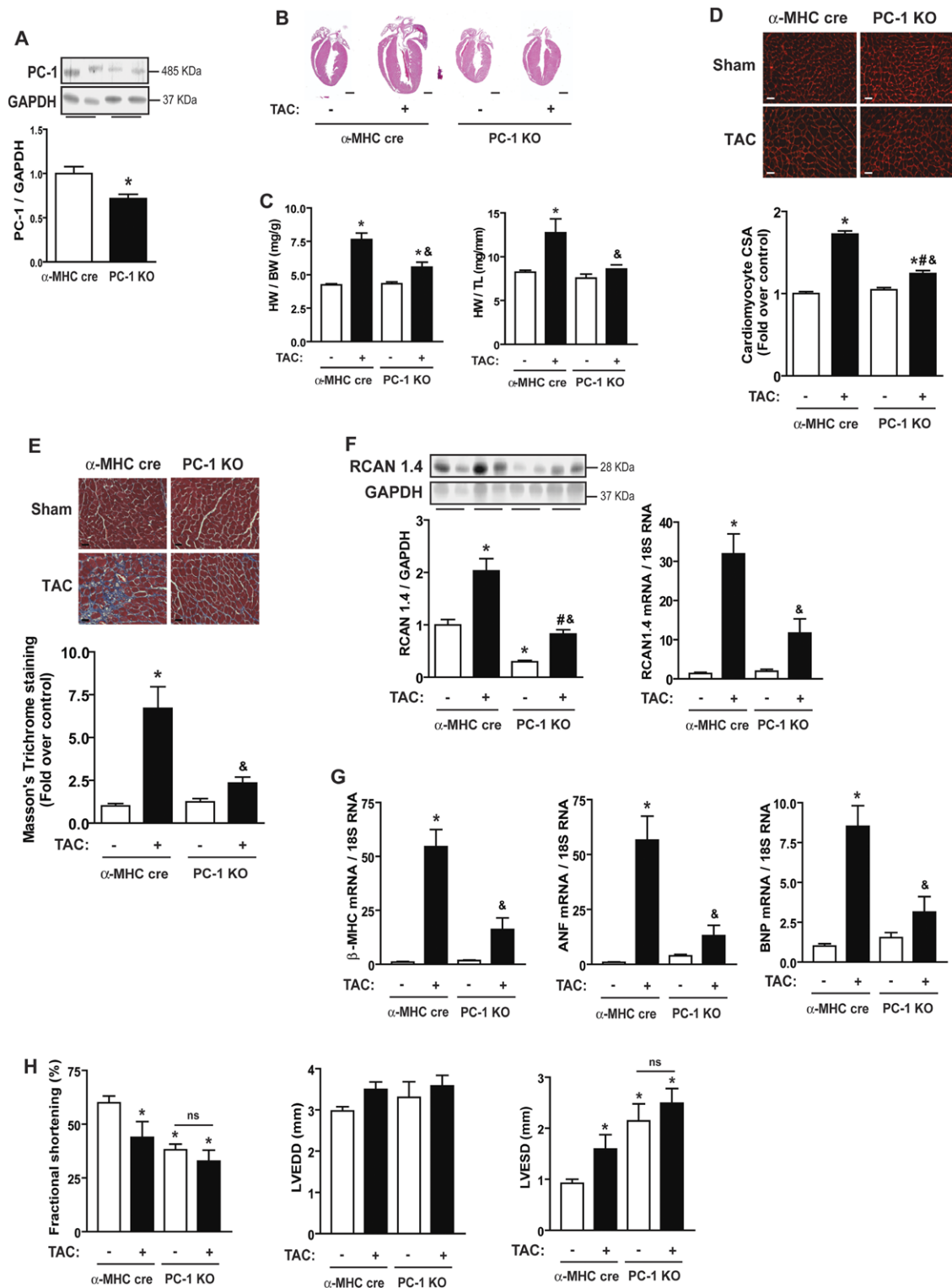


Figure 5. Cardiac hypertrophy is attenuated in polycystin-1 (PC-1) knockout (KO) mice. **A**, Representative PC-1 Western blot from the ventricular tissue of PC-1 KO mice and its densitometric quantification. **B**, Hematoxylin and eosin staining in 4-chamber heart sections after transverse aortic constriction (TAC). **C**, Heart weight/body weight (HW/BW) and heart weight/tibia length (HW/TL) ratios are depicted. Representative images of left ventricular cardiomyocytes (transverse section of the left ventricle) are shown as follows: **D**, Wheat germ agglutinin (red) and cross-sectional area (CSA) of cardiomyocytes quantified from at least 25 cells per section and 2 sections per group. **E**, Masson trichrome (blue) and densitometric analysis of the tissue sections. **F**, Representative Western blots of RCAN1.4 and GAPDH (top) with RCAN1.4/GAPDH depicted (bottom left). mRNA levels of RCAN1.4 are presented as RCAN1.4/18S ratio (bottom right). **G**, mRNA quantification of hypertrophic markers (β -myosin heavy chain [β -MHC], atrial natriuretic factor [ANF], brain natriuretic peptide [BNP]) is depicted. **H**, Ventricular function, quantified as percent fractional shortening (%FS; left) and ventricular dimensions (left ventricular end-diastolic dimension [LVEDD; center] and left ventricular end-systolic dimension [LVESD; right]), is depicted for hearts 3 weeks after sham or TAC surgery (α -myosin heavy chain [α -MHC]-cre, PC-1 KO mice). Scale bar, 150 μ m (**B**) and 20 μ m (**D** and **E**). Values are mean \pm SEM analyzed by the Welch test of 1-way ANOVA followed by the Tukey test (n=6–8). * P <0.05 vs α -MHC-cre; # P <0.05 vs PC-1 KO; & P <0.05 vs α -MHC-cre after TAC.

PC-1 KO animals developed normally, manifesting no apparent phenotype at birth. However, by 8 weeks of age, echocardiographic examination revealed a distinct defect in systolic function (Figure IIB in the online-only Data Supplement). Moreover, our results show that ventricular function in these animals remained persistently depressed at 15 weeks of age (Figure IIC in the online-only Data Supplement). Because it has been reported that mice haploinsufficient for the α 1C subunit manifest a similar phenotype,³³ we compared the levels of α 1C protein in control (α -MHC-cre) and PC-1 KO hearts. Interestingly, Western analysis revealed a significant decrease in α 1C LTCC protein abundance in PC-1 KO hearts (Figure IID in the online-only Data Supplement), consistent with a role for PC-1 in regulating LTCC levels and in the normal functioning of adult heart.

Next, we subjected mice (9–11 weeks old) to increased afterload by TAC. Both control (α -MHC-cre) and PC-1 KO mice were subjected to TAC or sham surgery, and structural, functional, and molecular events were evaluated at 3 weeks after surgery. As expected, TAC triggered an increase in the mass of the α -MHC-cre transgenic hearts compared with sham-operated controls (heart weight/body weight increased 80% from 4.2 ± 0.2 to 7.6 ± 1.4 mg/g; $P<0.001$; Figure 5B and 5C). Similar findings were observed when heart weight was normalized to tibia length (Figure 5C). In contrast, TAC surgery elicited no significant heart growth in PC-1 KO hearts (heart weight/body weight: sham, 4.3 ± 0.4 mg/g; TAC, 5.4 ± 1.0 mg/g; $P=NS$; Figure 5B and 5C). This blunting of load-induced growth was confirmed by heart weight/tibia length measurements (Figure 5C). These data support a model in which PC-1 is essential for the development of pressure overload–induced cardiac hypertrophy.

Examination of myocardial structure revealed the expected increases in cardiomyocyte cross-sectional area in TAC-stressed control heart, consistent with cardiomyocyte hypertrophy (Figure 5D). Those increases, however, were absent in the TAC-exposed PC-1 KO heart. TAC elicited significant fibrosis in the control heart, which was significantly ($P<0.05$) attenuated in the PC-1 KO heart (Figure 5E). These data provide further evidence for a requirement of PC-1, functioning as a mechanosensor, in stress-induced cardiac growth.

In control animals, TAC surgery triggered an increase in the steady-state levels of RCAN1.4 protein and mRNA levels of hypertrophic markers (β -MHC, atrial natriuretic factor, brain natriuretic peptide, RCAN1.4). These effects were blunted in the PC-1 KO animals (Figure 5F and 5G). No changes in PC-2 mRNA levels were detected in PC-1 KO mouse cardiac tissue under baseline conditions. Interestingly, both *Pkd-1* and *Pkd-2* mRNA levels were increased after TAC in control mice, and TAC-induced increases in PC-2 transcript were blunted in PC-1 KO mice (Figure IIE and IIF in the online-only Data Supplement). However, PC-2 protein levels manifested no significant change under these conditions (Figure IIG and IIH in the online-only Data Supplement).

Finally, we tested whether blunting of load-induced cardiac hypertrophy in PC-1 KO mice led to protection against cardiac dysfunction. PC-1 KO mice manifested baseline contractile dysfunction (fractional shortening: $40\pm 3\%$ for PC-1 KO versus $65\pm 4\%$ for wild-type mice; $P<0.0001$). TAC-triggered

ventricular dilation in control heart at 3 weeks was significantly exacerbated in the PC-1 KO heart (Figure 5H). Ventricular function 3 weeks after TAC surgery decreased significantly in both control and PC-1 KO animals, although the extent of decline was significantly greater in the PC-1 KO animals (fractional shortening: $33\pm 15\%$ for PC-1 KO versus $65\pm 4\%$ for wild-type mice; $P<0.0001$; Figure 5H).

Discussion

Mechanisms governing disease-related mechanotransduction in heart remain elusive, despite the fact that it is a proximal trigger of cellular events culminating in prevalent forms of disease. Here, we evaluated the role of PC-1, a molecule that is expressed in cardiomyocytes with a function that was unknown but is capable of serving as a mechanical sensor in other cell types. We report that PC-1 is required for stretch-induced cardiomyocyte hypertrophy in vitro and pressure overload–induced hypertrophy in vivo. PC-1 is required for normal contractile function at baseline. Mechanistically, PC-1 functions to stabilize LTCC protein, thereby promoting LTCC sarcolemmal localization and function. We go on to map this protein-stabilizing activity to the cytoplasmic C terminus of PC-1. Together, these data uncover a novel mechanism governing load-induced hypertrophic remodeling in heart.

Mechanotransduction and PC-1

Conversion of extracellular cues into intracellular biochemical responses is critical to a wide range of biological events. The heart is subject to stimuli, both physiological and pathological, that elicit a robust plasticity response.³ In particular, mechanical forces impinging on the cardiomyocyte trigger a host of biochemical, signaling, electrical, metabolic, and transcriptional events.³⁴ Whereas much is known about the intracellular events elicited by MS,³⁵ relatively little is known about how that stress is sensed and how it triggers intracellular events.

PC-1 is a large integral membrane glycoprotein with a long N-terminal extracellular domain, 11 transmembrane domains, and a short intracellular C-terminal tail. This 200-aa intracellular C terminus participates in signaling with other proteins, or after proteolytic cleavage, it can modulate pathways such as mammalian target of rapamycin, calcineurin/NFAT, Wnt, activator protein-1, and STAT6.^{5,31,36,37} PC-1 also interacts with PC-2, a Ca²⁺-regulated nonselective cation channel.^{7,38} PC-1 can also modulate levels of cytoplasmic Ca²⁺ through PC-2, inositol 1,4,5-trisphosphate receptor, or stromal interaction molecule-1 regulation.^{31,39}

Originally identified by positional cloning,⁴ PC-1 functions to transduce extracellular mechanical events in a number of cell types.^{5,7,9,31} In zebrafish, PC-2 loss of function results in cardiac dysfunction and atrioventricular conduction block.⁴⁰ Interestingly, the subcellular localization of PC-1 and PC-2 in cardiomyocytes remains uncertain, with some evidence pointing to both plasmalemmal and sarcoplasmic reticulum localization.⁴¹

MS is one of the primary stimuli to induce cardiac hypertrophy.⁴² Integrins, angiotensin-1 receptor, and stretch-activated ion channels have all been characterized as mechanosensors in cardiomyocytes,⁴³ but these findings remain conflicting, suggesting that other mechanosensors may also be present. PC-1 is a membrane protein best described as part of the primary

cilium in renal epithelial cells, serving to sense and transduce shear stress to modulate a variety of downstream pathways.^{5,31,36,37} However, PC-1 has also been suggested to work as a mechanosensor via other mechanisms.^{9–11}

We used 2 distinct *in vitro* models of mechanical stretch: hypo-osmotic stress and cyclic mechanical stretch. Hypo-osmotic stress has been used previously to impose static mechanical stretch, homologous to the stress of cyclic mechanical stretch.⁴⁴ In the latter, the degree of stretch used (20%) likely represents a pathological, as opposed to physiological, trigger.³⁰ Importantly, all of our observations in HS conditions were reproduced in the cyclic stretch model. Thus, our data point to an important role of PC-1 in mechanotransduction within cardiomyocytes.

Ca²⁺-Dependent Control of Cardiomyocyte Growth

Perturbations of intracellular Ca²⁺ signaling^{45,46} accompany many forms of heart disease and contribute to the pathogenesis of cardiac hypertrophy and failure. The LTCC is the major mediator of Ca²⁺ influx into cardiomyocytes and an important determinant of action potential morphology. The role of the LTCC, the proximal element in Ca²⁺ signaling, in the pathophysiology of cardiac hypertrophy remains incompletely characterized.

Intracellular Ca²⁺ metabolism and signaling are altered in both hypertrophic and failing hearts, contributing to disease pathogenesis.⁴⁷ Some of these changes have common features between the 2 phenotypes, whereas others are contrasting. In either case, altered Ca²⁺ handling contributes to the activation of several kinase and phosphatase cascades, including those involving mitogen-activated protein kinases, protein kinase C, and calcineurin.^{48,49} Together, such abnormal profiles of signaling lead to disturbances in gene regulation, which may promote disease progression.

Entry of a small amount of Ca²⁺ via LTCC triggers the release of much larger amounts of Ca²⁺ from intracellular stores.²⁶ As a result, PC-1–dependent governance of LTCC protein stability is likely to have an amplified impact on intracellular Ca²⁺ handling events. In addition, membrane impedance is relatively high during phase 2 of the action potential in many species, so changes in LTCC abundance have important effects on action potential morphology and duration.

The LTCC in heart comprises a large pore-forming subunit α 1C (also known as Cav1.2) plus the auxiliary subunits α 2- δ and β 2. In failing human ventricular myocytes, LTCC activity often exceeds that predicted from constant levels of α 1C transcript and protein, suggesting posttranslational regulation of the channel complex, possibly via phosphorylation.⁵⁰ This is the first report to uncover regulated control of LTCC subunit protein catabolic events.

Silencing the gene encoding α 1C results in embryonic lethality.⁵¹ Deletion of 1 copy of the α 1C subunit gene (*Cacna1c*) results in decreased steady-state levels of α 1C protein and a decrease in LTCC activity in adult cardiomyocytes.³³ Animals harboring this heterozygous genotype display cardiac dysfunction by 3 to 10 weeks of age with increased systolic chamber size. Interestingly, we report here that mice harboring cardiomyocyte-specific loss of PC-1 manifest a similar phenotype with a significant decrease in ventricular contractile function by 8 to 10 weeks, driven by an increase in

LVESD. Steady-state levels of α 1C in these mice are significantly low, suggesting that the phenotype derives, at least in part, from a decrease in LTCC activity.

LTCC-Dependent Control of Cardiomyocyte Hypertrophy

A multitude of studies have linked Ca²⁺ influx from LTCCs with the intracellular signaling and gene regulatory events that trigger cardiac hypertrophy and disease.³⁵ Consistent with this idea, LTCC blockers can inhibit pressure overload–induced hypertrophy.³³ Here, we report that PC-1 suppresses proteasome-dependent degradation of the α 1C subunit protein. Interestingly, this decrease had no effect on phenylephrine-induced hypertrophy, consistent with the notion that β -adrenergic stimulation of LTCC activity stems mainly from increases in the open state of the channel rather than channel abundance.⁵² In contrast, PC-1 knockdown blunted the hypertrophy induced mechanically by HS or MS treatment. HS treatment led to an increase in α 1C steady-state levels within an hour of treatment, as well as LTCC formation, as evidenced by increased association with the β subunit and surface localization of α 1C protein. We also tested for a role of ROS in the stabilization of LTCC protein after stretch, but in fact, antioxidant (trolox) had no effect. These data suggest that the stabilization of α 1C is a proximal trigger of the hypertrophic response. Furthermore, they uncover a previously unrecognized role for regulated proteasome-dependent LTCC degradation in the hypertrophic response.

Cardiomyocyte-specific deletion of PC-1 *in vivo* resulted in attenuation of the hypertrophic response to pressure overload. Consistent with our *in vitro* findings, PC-1 KO resulted in lower steady-state α 1C levels *in vivo*. These findings fit well with earlier studies that reported blunting of pressure overload–induced hypertrophy by pharmacological inhibition of LTCC activity or genetic downregulation of the β 2 subunit.^{53,54}

Goonasekera et al³³ reported that mice haploinsufficient for α 1C manifest a slightly exaggerated hypertrophic response to TAC or other stressors. It remains unclear why these mice mount a hypertrophic response but PC-1 KO animals (with a similar decrease in α 1C abundance) do not. One possibility is that α 1C^{+/–} mice retain the ability to stabilize the remaining α 1C protein, resulting in an increase in LTCC activity relative to sham-operated controls. Alternatively, PC-1 may function through additional pathways to influence the response to pressure-overload stress.

Although hypertrophy has been associated in a number of studies with increases in LTCC activity, increased protein levels of LTCC have not been observed.^{55–57} In our hands, 3 weeks after TAC, α 1C protein levels show no increase from baseline in either control or PC-1 KO hearts (Figure IIIA in the online-only Data Supplement). Our *in vitro* data suggest a model of PC-1–dependent increases in LTCC steady-state levels that correlate with the hypertrophic response. Interestingly, protein levels of β 2 increase after TAC only in PC-1 KO mice, perhaps as a compensatory response to diminished LTCC levels (Figure IIIB and IIIC in the online-only Data Supplement).

The specific mechanism whereby PC-1 stabilizes α 1C protein remains unclear. PC-1 KO hearts manifest a decrease in α 1C levels, consistent with a role for PC-1 in regulating protein stability. The effect is rapid, occurring within 1 hour of stress

induction, and appears independent of a direct role for PC-1 in transcription. Localization of PC-1 to the plasma membrane and the evidence of physical proximity from the proximity ligation assay suggest that the mechanism could be direct; however PC-1 has also been implicated in a number of downstream pathways, including AKT activation,⁵⁸ which could represent an indirect mechanism for LTCC stabilization. Interestingly, 1 report documented the existence of an endogenous, 100-kDa PC-1 cleavage product that functions to reduce SOCE via direct inhibition of stromal interaction molecule-1 translocation.⁵⁹

Conclusions

We report here that PC-1 serves as a mechanosensor in cardiomyocytes and governs a novel mechanism of regulated degradation of LTCC protein. This cascade participates importantly in stress-induced hypertrophic growth triggered by hypotonic stress, MS, and increased afterload. These findings uncover a previously unrecognized mechanism of stress-induced mechanotransduction, opening the potential prospect for therapeutic manipulation. Going forward, future studies will define mechanisms whereby the C-terminal domain of PC-1 regulates proteasome-dependent LTCC catabolism.

Acknowledgments

We sincerely thank everyone in the Hill and Lavandero laboratories for discussion and constructive criticism. Special thanks go to Yongli Kong and Fidel Albornoz for excellent technical assistance.

Sources of Funding

This work was supported by grants from the National Institutes of Health (HL-120732, Dr Hill; HL-100401, Dr Hill; HL-097768, Dr Rothermel; HL-072016; Dr Rothermel; DK-54053, Dr Somlo), American Heart Association (14SFRN20510023, Dr Hill; 14SFRN20670003; Dr Hill), Fondation Leducq (11CVD04), and Cancer Prevention and Research Institute of Texas (RP110486P3); by the PEW Latin American Fellows Program in the Biomedical Science (A.C.); by Fondo Nacional de Desarrollo Científico y Tecnológico, FONDECYT (3110039, 1150887 to Dr Pedrozo; 11130267 to A.C.-F.); by FONDAP (15130011 to Drs Lavandero, Pedrozo, and Hill); and by REDES 120003 (to Drs Lavandero and Hill) from the Comisión Nacional de Investigación Científica y Tecnológica (CONICYT), Santiago, Chile, Programa U-INICIA Concurso de Reforzamiento de Inserción Productiva de Nuevos Académicos VID 2014, Universidad de Chile (Z.P.).

Disclosures

None.

References

- Dobner S, Amadi OC, Lee RT. Cardiovascular mechanotransduction. In: *Muscle Fundamental Biology and Mechanisms of Disease*. Academic Press: Amsterdam. 2012;1:Chap. 14. <https://www.elsevier.com/books/muscle-2-volume-set/hill/978-0-12-381510-1>. Accessed May 5, 2015.
- Grossman W, Jones D, McLaurin LP. Wall stress and patterns of hypertrophy in the human left ventricle. *J Clin Invest*. 1975;56:56–64. doi: 10.1172/JCI108079.
- Hill JA, Olson EN. Cardiac plasticity. *N Engl J Med*. 2008;358:1370–1380. doi: 10.1056/NEJMr072139.
- Zhou J. Polycystins and primary cilia: primers for cell cycle progression. *Annu Rev Physiol*. 2009;71:83–113. doi: 10.1146/annurev.physiol.70.113006.100621.
- Igarashi P, Somlo S. Genetics and pathogenesis of polycystic kidney disease. *J Am Soc Nephrol*. 2002;13:2384–2398.
- Torres VE, Harris PC. Mechanisms of disease: autosomal dominant and recessive polycystic kidney diseases. *Nat Clin Pract Nephrol*. 2006;2:40–55; quiz 55. doi: 10.1038/ncpneph0070.

- Wilson PD. Polycystin: new aspects of structure, function, and regulation. *J Am Soc Nephrol*. 2001;12:834–845.
- Dalagiorou G, Basdra EK, Papavassiliou AG. Polycystin-1: function as a mechanosensor. *Int J Biochem Cell Biol*. 2010;42:1610–1613. doi: 10.1016/j.biocel.2010.06.017.
- Forman JR, Qamar S, Paci E, Sandford RN, Clarke J. The remarkable mechanical strength of polycystin-1 supports a direct role in mechanotransduction. *J Mol Biol*. 2005;349:861–871. doi: 10.1016/j.jmb.2005.04.008.
- Qian F, Wei W, Germino G, Oberhauser A. The nanomechanics of polycystin-1 extracellular region. *J Biol Chem*. 2005;280:40723–40730. doi: 10.1074/jbc.M509650200.
- Forman JR, Yew ZT, Qamar S, Sandford RN, Paci E, Clarke J. Non-native interactions are critical for mechanical strength in PKD domains. *Structure*. 2009;17:1582–1590. doi: 10.1016/j.str.2009.09.013.
- Benitah JP, Alvarez JL, Gómez AM. L-type Ca(2+) current in ventricular cardiomyocytes. *J Mol Cell Cardiol*. 2010;48:26–36. doi: 10.1016/j.yjmcc.2009.07.026.
- Puri S, Magenheimer BS, Maser RL, Ryan EM, Zien CA, Walker DD, Wallace DP, Hempson SJ, Calvet JP. Polycystin-1 activates the calcineurin/NFAT (nuclear factor of activated T-cells) signaling pathway. *J Biol Chem*. 2004;279:55455–55464. doi: 10.1074/jbc.M402905200.
- Battiprolu PK, Hojavey B, Jiang N, Wang ZV, Luo X, Iglewski M, Shelton JM, Gerard RD, Rothermel BA, Gillette TG, Lavandero S, Hill JA. Metabolic stress-induced activation of FoxO1 triggers diabetic cardiomyopathy in mice. *J Clin Invest*. 2012;122:1109–1118. doi: 10.1172/JCI60329.
- Shibazaki S, Yu Z, Nishio S, Tian X, Thomson RB, Mitobe M, Louvi A, Velazquez H, Ishibe S, Cantley LG, Igarashi P, Somlo S. Cyst formation and activation of the extracellular regulated kinase pathway after kidney specific inactivation of Pkd1. *Hum Mol Genet*. 2008;17:1505–1516. doi: 10.1093/hmg/ddn039.
- Hill JA, Karimi M, Kutschke W, Davisson RL, Zimmerman K, Wang Z, Kerber RE, Weiss RM. Cardiac hypertrophy is not a required compensatory response to short-term pressure overload. *Circulation*. 2000;101:2863–2869.
- Contreras-Ferrat A, Llanos P, Vasquez C, Espinosa A, Osorio-Fuentealba C, Arias-Calderon M, Lavandero S, Klip A, Hidalgo C, Jaimovich E. Insulin elicits a ROS-activated and an IP(3)-dependent Ca(2+)(+) release, which both impinge on GLUT4 translocation. *J Cell Sci*. 2014;127:1911–1923.
- Dalagiorou G, Piperi C, Georgopoulou U, Adamopoulos C, Basdra EK, Papavassiliou AG. Mechanical stimulation of polycystin-1 induces human osteoblastic gene expression via potentiation of the calcineurin/NFAT signaling axis. *Cell Mol Life Sci*. 2013;70:167–180. doi: 10.1007/s00018-012-1164-5.
- Molkentin JD, Lu JR, Antos CL, Markham B, Richardson J, Robbins J, Grant SR, Olson EN. A calcineurin-dependent transcriptional pathway for cardiac hypertrophy. *Cell*. 1998;93:215–228.
- Rakesh K, Yoo B, Kim IM, Salazar N, Kim KS, Rockman HA. Beta-arrestin-biased agonism of the angiotensin receptor induced by mechanical stress. *Sci Signal*. 2010;3:ra46. doi: 10.1126/scisignal.2000769.
- Sanna B, Bueno OF, Dai YS, Wilkins BJ, Molkentin JD. Direct and indirect interactions between calcineurin-NFAT and MEK1-extracellular signal-regulated kinase 1/2 signaling pathways regulate cardiac gene expression and cellular growth. *Mol Cell Biol*. 2005;25:865–878. doi: 10.1128/MCB.25.3.865-878.2005.
- Viola HM, Macdonald WA, Tang H, Hool LC. The L-type Ca(2+) channel as a therapeutic target in heart disease. *Curr Med Chem*. 2009;16:3341–3358.
- Zobel C, Rana OR, Saygili E, Bölk B, Saygili E, Diedrichs H, Reuter H, Frank K, Müller-Ehmsen J, Pfitzer G, Schwinger RH. Mechanisms of Ca²⁺-dependent calcineurin activation in mechanical stretch-induced hypertrophy. *Cardiology*. 2007;107:281–290. doi: 10.1159/000099063.
- Luo X, Hojavey B, Jiang N, Wang ZV, Tandan S, Rakalín A, Rothermel BA, Gillette TG, Hill JA. Stim1-dependent store-operated Ca²⁺ entry is required for pathological cardiac hypertrophy. *J Mol Cell Cardiol*. 2012;52:136–147.
- Sarsero D, Fujiwara T, Molenaar P, Angus JA. Human vascular to cardiac tissue selectivity of L- and T-type calcium channel antagonists. *Br J Pharmacol*. 1998;125:109–119. doi: 10.1038/sj.bjp.0702045.
- Bodi I, Mikala G, Koch SE, Akhter SA, Schwartz A. The L-type calcium channel in the heart: the beat goes on. *J Clin Invest*. 2005;115:3306–3317. doi: 10.1172/JCI27167.
- Hullin R, Khan IF, Wirtz S, Mohacs P, Varadi G, Schwartz A, Herzig S. Cardiac L-type calcium channel beta-subunits expressed in human heart have differential effects on single channel characteristics. *J Biol Chem*. 2003;278:21623–21630. doi: 10.1074/jbc.M211164200.
- Zhao Y, Xu J, Gong J, Qian L. L-type calcium channel current up-regulation by chronic stress is associated with increased alpha(1c) subunit expression

- in rat ventricular myocytes. *Cell Stress Chaperones*. 2009;14:33–41. doi: 10.1007/s12192-008-0052-2.
29. Altier C, Garcia-Caballero A, Simms B, You H, Chen L, Walcher J, Tedford HW, Hermosilla T, Zamponi GW. The α 1 subunit prevents RFP2-mediated ubiquitination and proteasomal degradation of L-type channels. *Nat Neurosci*. 2011;14:173–180.
 30. Prosser BL, Ward CW, Lederer WJ. X-ROS signalling is enhanced and graded by cyclic cardiomyocyte stretch. *Cardiovasc Res*. 2013;98:307–314. doi: 10.1093/cvr/cvt066.
 31. Chapin HC, Caplan MJ. The cell biology of polycystic kidney disease. *J Cell Biol*. 2010;191:701–710. doi: 10.1083/jcb.201006173.
 32. Chauvet V, Tian X, Husson H, Grimm DH, Wang T, Hiesberger T, Hiesberger T, Igarashi P, Bennett AM, Ibraghimov-Beskrovnaia O, Somlo S, Caplan MJ. Mechanical stimuli induce cleavage and nuclear translocation of the polycystin-1 C terminus. *J Clin Invest*. 2004;114:1433–1443. doi: 10.1172/JCI21753.
 33. Goonasekera SA, Hammer K, Auger-Messier M, Bodi I, Chen X, Zhang H, Reiken S, Elrod JW, Correll RN, York AJ, Sargent MA, Hofmann F, Moosmang S, Marks AR, Houser SR, Bers DM, Molkentin JD. Decreased cardiac L-type Ca^{2+} channel activity induces hypertrophy and heart failure in mice. *J Clin Invest*. 2012;122:280–290.
 34. McCain ML, Parker KK. Mechanotransduction: the role of mechanical stress, myocyte shape, and cytoskeletal architecture on cardiac function. *Pflugers Arch*. 2011;462:89–104. doi: 10.1007/s00424-011-0951-4.
 35. Burchfield JS, Xie M, Hill JA. Pathological ventricular remodeling: mechanisms: part 1 of 2. *Circulation*. 2013;128:388–400. doi: 10.1161/CIRCULATIONAHA.113.001878.
 36. Wei W, Hackmann K, Xu H, Germino G, Qian F. Characterization of cis-auto-proteolysis of polycystin-1, the product of human polycystic kidney disease 1 gene. *J Biol Chem*. 2007;282:21729–21737. doi: 10.1074/jbc.M703218200.
 37. Dere R, Wilson PD, Sandford RN, Walker CL. Carboxy terminal tail of polycystin-1 regulates localization of TSC2 to repress mTOR. *PLoS One*. 2010;5:e9239. doi: 10.1371/journal.pone.0009239.
 38. Sutters M. The pathogenesis of autosomal dominant polycystic kidney disease. *Nephron Exp Nephrol*. 2006;103:e149–e155. doi: 10.1159/000093216.
 39. Santoso NG, Cebotaru L, Guggino WB. Polycystin-1, 2, and STIM1 interact with IP(3)R to modulate ER Ca release through the PI3K/Akt pathway. *Cell Physiol Biochem*. 2011;27:715–726. doi: 10.1159/000330080.
 40. Paavola J, Schliffke S, Rossetti S, Kuo IY, Yuan S, Sun Z, Harris PC, Torres VE, Ehrlich BE. Polycystin-2 mutations lead to impaired calcium cycling in the heart and predispose to dilated cardiomyopathy. *J Mol Cell Cardiol*. 2013;58:199–208. doi: 10.1016/j.yjmcc.2013.01.015.
 41. Grimm DH, Cai Y, Chauvet V, Rajendran V, Zeltner R, Geng L, Avner ED, Sweeney W, Somlo S, Caplan MJ. Polycystin-1 distribution is modulated by polycystin-2 expression in mammalian cells. *J Biol Chem*. 2003;278:36786–36793. doi: 10.1074/jbc.M306536200.
 42. Ruwhof C, van der Laarse A. Mechanical stress-induced cardiac hypertrophy: mechanisms and signal transduction pathways. *Cardiovasc Res*. 2000;47:23–37.
 43. Sadoshima J, Izumo S. The cellular and molecular response of cardiac myocytes to mechanical stress. *Annu Rev Physiol*. 1997;59:551–571. doi: 10.1146/annurev.physiol.59.1.551.
 44. Tang W, Strachan RT, Lefkowitz RJ, Rockman HA. Allosteric modulation of beta-arrestin-biased angiotensin II type 1 receptor signaling by membrane stretch. *J Biol Chem*. 2014;289:28271–28283.
 45. Wickenden AD, Kaprielian R, Kassiri Z, Tsoporis JN, Tushima R, Fishman GI, Backx PH. The role of action potential prolongation and altered intracellular calcium handling in the pathogenesis of heart failure. *Cardiovasc Res*. 1998;37:312–323.
 46. Frey N, McKinsey TA, Olson EN. Decoding calcium signals involved in cardiac growth and function. *Nat Med*. 2000;6:1221–1227. doi: 10.1038/81321.
 47. Luo M, Anderson ME. Mechanisms of altered Ca^{2+} handling in heart failure. *Circ Res*. 2013;113:690–708.
 48. Molkentin JD. Calcineurin-NFAT signaling regulates the cardiac hypertrophic response in coordination with the MAPKs. *Cardiovasc Res*. 2004;63:467–475. doi: 10.1016/j.cardiores.2004.01.021.
 49. Lou Q, Janardhan A, Efimov IR. Remodeling of calcium handling in human heart failure. *Adv Exp Med Biol*. 2012;740:1145–1174. doi: 10.1007/978-94-007-2888-2_52.
 50. Schröder F, Handrock R, Beuckelmann DJ, Hirt S, Hullin R, Priebe L, Schwinger RH, Weil J, Herzig S. Increased availability and open probability of single L-type calcium channels from failing compared with nonfailing human ventricle. *Circulation*. 1998;98:969–976.
 51. Karnabi E, Qu Y, Mancarella S, Boutjdir M. Rescue and worsening of congenital heart block-associated electrocardiographic abnormalities in two transgenic mice. *J Cardiovasc Electrophysiol*. 2011;22:922–930. doi: 10.1111/j.1540-8167.2011.02032.x.
 52. van der Heyden MA, Wijnhoven TJ, Opthof T. Molecular aspects of adrenergic modulation of cardiac L-type Ca^{2+} channels. *Cardiovasc Res*. 2005;65:28–39. doi: 10.1016/j.cardiores.2004.09.028.
 53. Liao Y, Asakura M, Takashima S, Ogai A, Asano Y, Asanuma H, Minamino T, Tomoike H, Hori M, Kitakaze M. Benidipine, a long-acting calcium channel blocker, inhibits cardiac remodeling in pressure-overloaded mice. *Cardiovasc Res*. 2005;65:879–888. doi: 10.1016/j.cardiores.2004.11.006.
 54. Semsarian C, Ahmad I, Giewat M, Georgakopoulos D, Schmitt JP, McConnell BK, Reiken S, Mende U, Marks AR, Kass DA, Seidman CE, Seidman JG. The L-type calcium channel inhibitor diltiazem prevents cardiomyopathy in a mouse model. *J Clin Invest*. 2002;109:1013–1020. doi: 10.1172/JCI14677.
 55. Wang Z, Kutschke W, Richardson KE, Karimi M, Hill JA. Electrical remodeling in pressure-overload cardiac hypertrophy: role of calcineurin. *Circulation*. 2001;104:1657–1663.
 56. Yatani A, Honda R, Tymitz KM, Lalli MJ, Molkentin JD. Enhanced Ca^{2+} channel currents in cardiac hypertrophy induced by activation of calcineurin-dependent pathway. *J Mol Cell Cardiol*. 2001;33:249–259. doi: 10.1006/jmcc.2000.1296.
 57. Gao H, Wang F, Wang W, Makarewich CA, Zhang H, Kubo H, Berretta RM, Barr LA, Molkentin JD, Houser SR. Ca^{2+} influx through L-type Ca^{2+} channels and transient receptor potential channels activates pathological hypertrophy signaling. *J Mol Cell Cardiol*. 2012;53:657–667. doi: 10.1016/j.yjmcc.2012.08.005.
 58. Boca M, Distefano G, Qian F, Bhunia AK, Germino GG, Boletta A. Polycystin-1 induces resistance to apoptosis through the phosphatidylinositol 3-kinase/Akt signaling pathway. *J Am Soc Nephrol*. 2006;17:637–647. doi: 10.1681/ASN.2005050534.
 59. Woodward OM, Li Y, Yu S, Greenwell P, Wodarczyk C, Boletta A, Guggino WB, Qian F. Identification of a polycystin-1 cleavage product, P100, that regulates store operated Ca^{2+} entry through interactions with STIM1. *PLoS One*. 2010;5:e12305. doi: 10.1371/journal.pone.0012305.

CLINICAL PERSPECTIVE

The myocardium reacts to physical stimuli—pressure, stretch, and shear stress—with a variety of molecular responses, culminating in adaptive growth or disease-related remodeling. A central response of the cell to such stimuli is changes in the handling of intracellular Ca^{2+} . How physical signals at the cell surface are transduced to govern changes in intracellular Ca^{2+} remains poorly characterized. Here, we report that the protein polycystin-1 (PC-1), a molecule implicated in polycystic kidney disease, is expressed in cardiac myocytes, serving as a major mechanism of mechanotransduction. We report that PC-1 is required for stretch-induced cardiomyocyte hypertrophy in vitro and pressure overload-induced hypertrophy in vivo. PC-1 is required for normal contractile performance at baseline. Mechanistically, PC-1 functions to stabilize Ca^{2+} channel protein stability, thereby promoting channel localization to the cell surface membrane and channel function. We go on to map this protein-stabilizing activity to the cytoplasmic C terminus of PC-1. Together, these data uncover a novel mechanism governing load-induced hypertrophic remodeling in heart.

Polycystin-1 Is a Cardiomyocyte Mechanosensor That Governs L-Type Ca²⁺ Channel Protein Stability

Zully Pedrozo, Alfredo Criollo, Pavan K. Battiprolu, Cyndi R. Morales, Ariel Contreras-Ferrat, Carolina Fernández, Nan Jiang, Xiang Luo, Michael J. Caplan, Stefan Somlo, Beverly A. Rothermel, Thomas G. Gillette, Sergio Lavandero and Joseph A. Hill

Circulation. 2015;131:2131-2142; originally published online April 17, 2015;
doi: 10.1161/CIRCULATIONAHA.114.013537

Circulation is published by the American Heart Association, 7272 Greenville Avenue, Dallas, TX 75231
Copyright © 2015 American Heart Association, Inc. All rights reserved.
Print ISSN: 0009-7322. Online ISSN: 1524-4539

The online version of this article, along with updated information and services, is located on the
World Wide Web at:

<http://circ.ahajournals.org/content/131/24/2131>

Data Supplement (unedited) at:

<http://circ.ahajournals.org/content/suppl/2015/04/17/CIRCULATIONAHA.114.013537.DC1.html>

Permissions: Requests for permissions to reproduce figures, tables, or portions of articles originally published in *Circulation* can be obtained via RightsLink, a service of the Copyright Clearance Center, not the Editorial Office. Once the online version of the published article for which permission is being requested is located, click Request Permissions in the middle column of the Web page under Services. Further information about this process is available in the [Permissions and Rights Question and Answer](#) document.

Reprints: Information about reprints can be found online at:
<http://www.lww.com/reprints>

Subscriptions: Information about subscribing to *Circulation* is online at:
<http://circ.ahajournals.org/subscriptions/>

ONLINE DATA SUPPLEMENT

Polycystin-1 is a Cardiomyocyte Mechanosensor that Governs L-type Ca²⁺ Channel Protein Stability

Zully Pedrozo, PhD^{1,2,7}; Alfredo Criollo, PhD^{3,7}; Pavan K. Battiprolu, PhD⁷;
Cyndi R. Morales, BS⁷; Ariel Contreras, PhD¹; Carolina Fernández, MSc¹;
Nan Jiang, MSc⁷; Xiang Luo, MD, PhD⁷; Michael J. Caplan, MD, PhD⁴;
Stefan Somlo, MD^{5,6}; Beverly A. Rothermel, PhD^{7,8}; Thomas G. Gillette, PhD⁷;
Sergio Lavandero, PhD^{1,2,7,#}; Joseph A. Hill, MD, PhD^{7,8,#}

¹Advanced Center for Chronic Diseases (ACCDiS) & Centro de Estudios Moleculares de la Célula (CMEC), Facultad de Medicina & Facultad de Ciencias Químicas y Farmacéuticas;
²Instituto de Ciencias Biomédicas, Facultad de Medicina; ³Instituto de Investigación en Ciencias Odontológicas, Facultad de Odontología, Universidad de Chile, Santiago, Chile;
Departments of ⁴Cellular and Molecular Physiology, ⁵Internal Medicine, and ⁶Genetics, Yale University School of Medicine, New Haven, CT; ⁷Division of Cardiology, Department of Internal Medicine, and the ⁸Department of Molecular Biology, University of Texas Southwestern Medical Center, Dallas, TX

Running title: PC-1-dependent mechanotransduction in heart

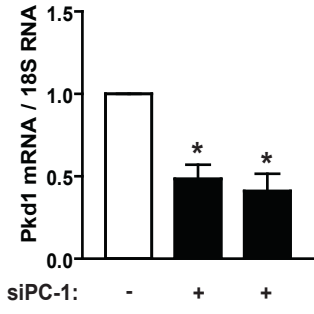
Correspondence to:

Joseph A. Hill, MD, PhD, Cardiology Division, Department of Internal Medicine
UT Southwestern Medical Center, 6000 Harry Hines Blvd, Dallas, TX 75390-8573
(joseph.hill@utsouthwestern.edu);

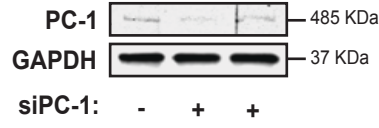
or Sergio Lavandero, PhD, Advanced Center for Chronic Diseases (ACCDiS),
Facultad de Ciencias Químicas & Facultad de Medicina,
Universidad de Chile, Olivos 1007, Santiago 8380492, Chile (slavander@uchile.cl).

Supplementary Figure I

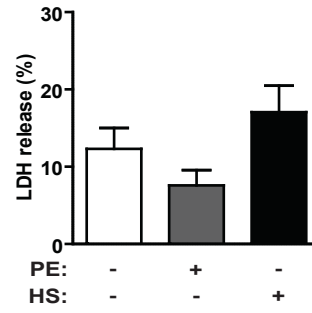
A



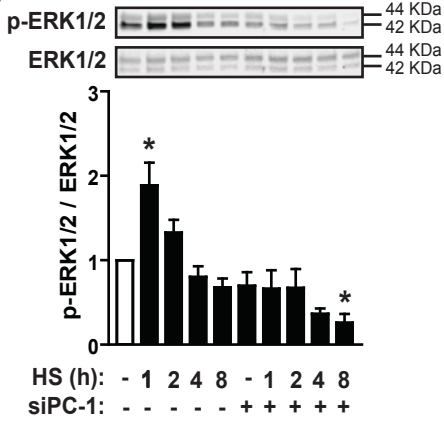
B



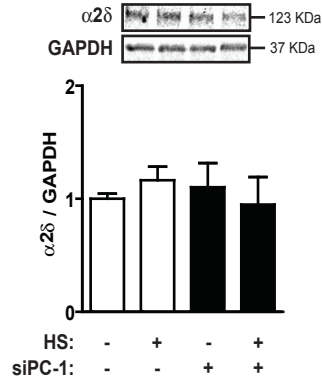
C



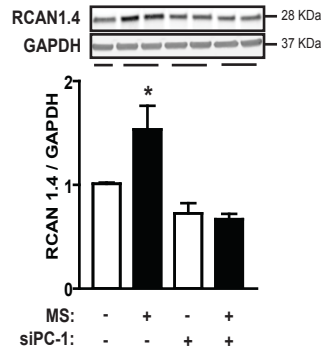
D



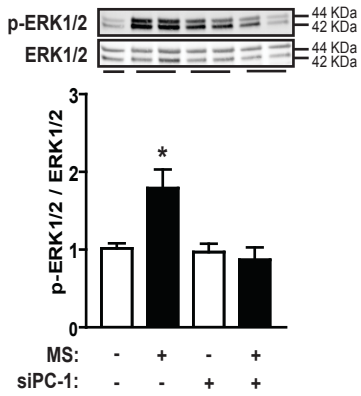
E



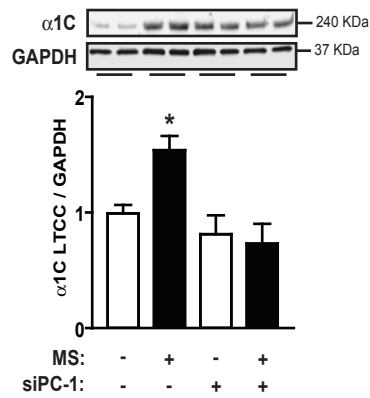
F



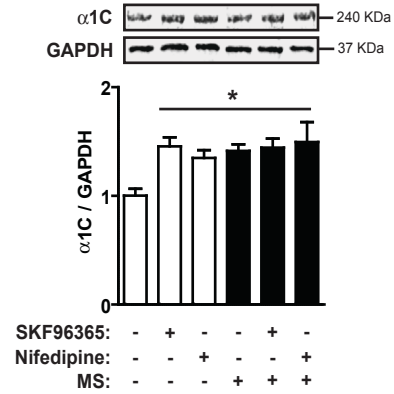
G



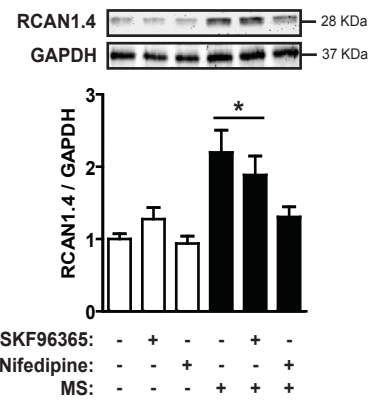
H



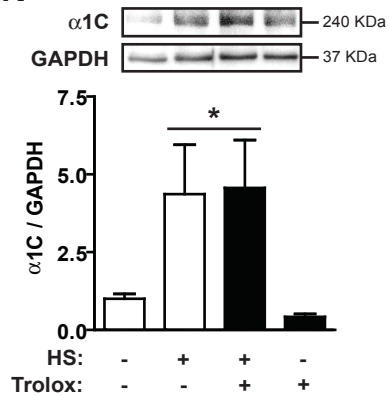
I



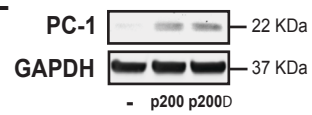
J



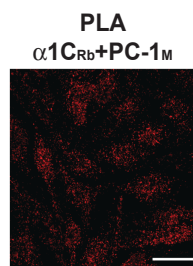
K



L

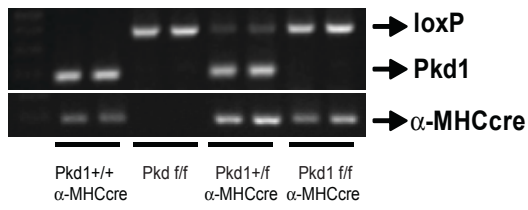


M

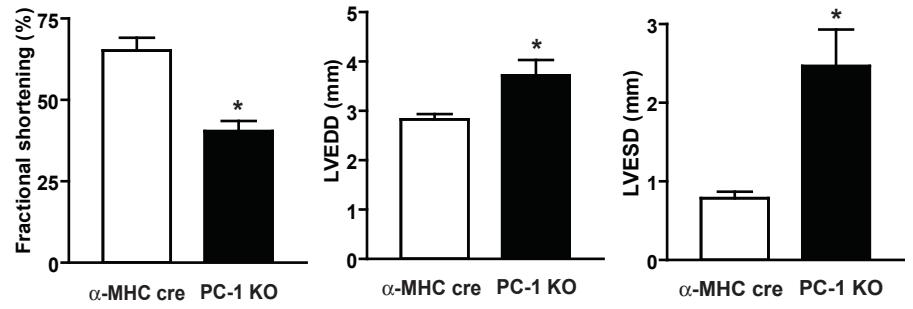


Supplementary Figure II.

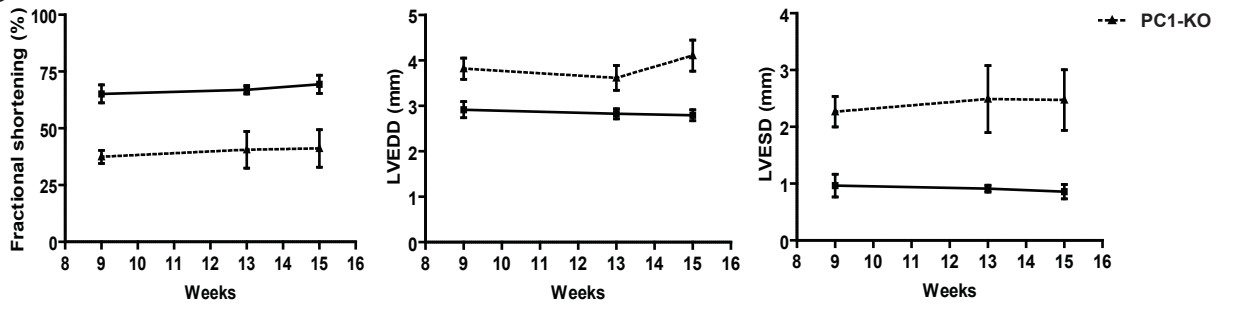
A



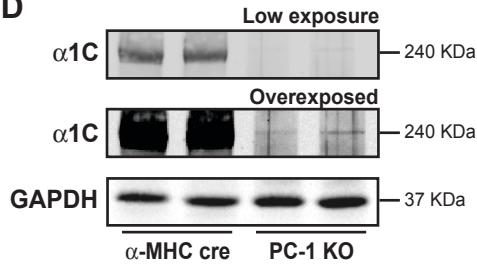
B



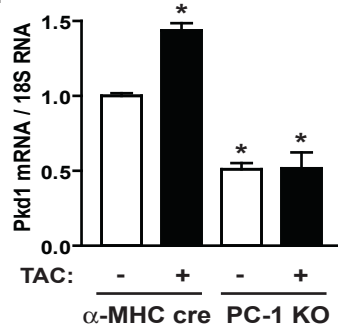
C



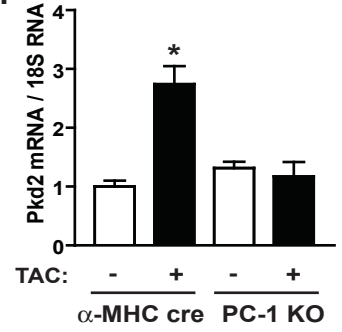
D



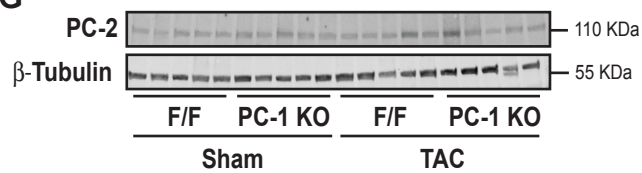
E



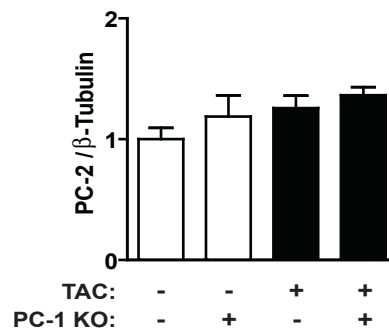
F



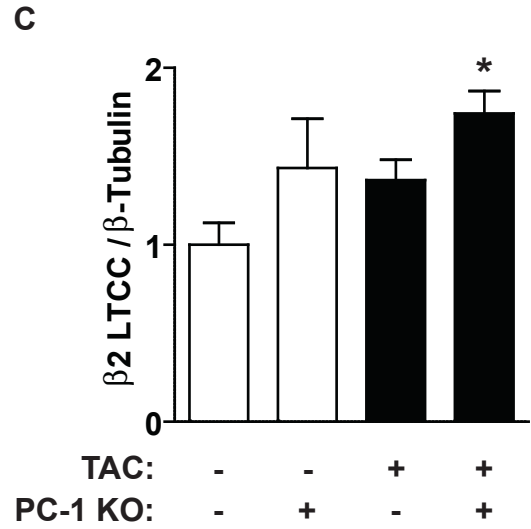
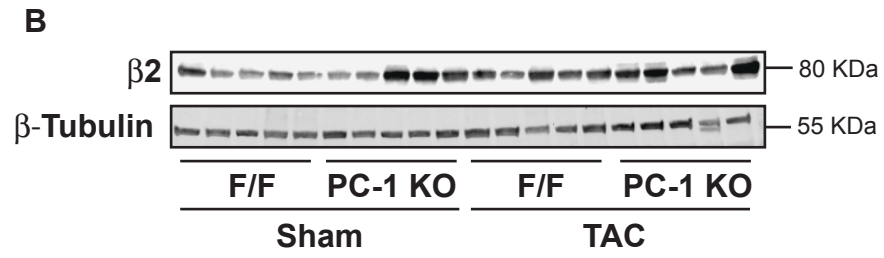
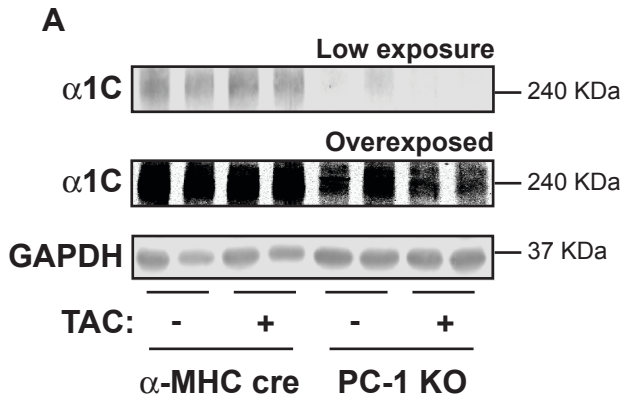
G



H



Supplementary Figure III.



Supplementary Table 1

Primer pairs used for Pkd-1 genotyping by PCR

Gene	Primer pair	
	Forward (5'-3')	Reverse (5'-3')
<i>Mouse</i>		
LOX	ccgctgtgtctcagtgccctg	caagagggcctttcttgctg
CRE	gatttcgaccagggttcgttc	gctaaccagcgttttcgttc

Supplementary Table 2

Primer pairs used for quantitative RT-PCR

Gene	Primer pair	
	Forward (5'-3')	Reverse (5'-3')
Mouse		
18S RNA	cggacaggattgacagattg	caaatcgctccaccaactaa
β -MHC	aagcagcagttggatgagcg	cctcgatgctgcctgaagc
ANF	cttctcctcgtcttggcct	ctgcttcctcagctgtctca
BNP	catggatctcctgaaggtgc	cctcaagagctgtctctgg
Pkd-1	gccatccagcacttcttagt	gagaagccgatccacacatc
Pkd-2	tgtgtggtcaggttattggcg	gccaggaagaaatcaaaggc
RCAN 1.4	cccgtgaaaaagcagaatgc	tccttgcatatgttctgaagaggg
α 1C	gttctggattgctgcgaga	aagaaatgcagcaacagccg
Rat		
18S RNA	aaacggctaccacatccaag	cctccaatggatcctcgta
β -MHC	ctgactgaacagctgggctc	aactctggaggctcttctact
RCAN 1.4	gacccgcgcgtgttc	tgatcatatgttctgaagaggattc
Pkd-1	gccatccagcacttcttagt	gaaaagccgatccacacgctc
Pkd-2	tgtgtggtcaggttattgggt	gccaggaagaaatcaaaggc
α 1C	agcaactccctcagacgtttg	gcttctcatgggacggtgat

Supplementary Figures

Figure I. A, *Pkd-1* mRNA levels from cardiomyocytes transfected with sequence-independent siRNA constructs targeting PC-1 (siPC-1) are depicted. B, PC-1 protein levels in cardiomyocytes transfected with 2 different, sequence-independent siRNAs. C, Cardiomyocyte death after exposure to phenylephrine (PE) or HS stimulation. Lactate dehydrogenase (LDH) activity was measured, and the results are shown as percent of LDH release in the culture medium. D, Representative Western blot for p-ERK1/2 and total ERK1/2 (above) and pERK1/2 / ERK1/2 ratio (below) in siPC-1 and controls cells. E, Representative Western blot for $\alpha 2\delta$ and quantification analysis in the bar graph. F, Western blots for RCAN1.4 and GAPDH (above) and quantification after mechanical stress (MS) stimulation (2 h). G, pERK1/2 and total ERK1/2 in control and siPC-1 cells stimulated with MS. H, $\alpha 1C$ protein levels after MS in control and siPC-1 cells. $\alpha 1C$ (I) and RCAN1.4 (J) representative Western blots after MS in presence of a SOCE inhibitor, SKF96365 or nifedipine and their corresponding quantifications. K, Representative Western blot for $\alpha 1C$ and densitometric analysis of cardiomyocytes stimulated with HS in presence of trolox. L, Western blot for PC-1 from NRVMs over-expressing PC-1 C-terminal peptide (p200) or the C-terminal peptide lacking the nuclear localization signal (p200 Δ). M, Duolink protein-protein interaction assay for PC-1 and $\alpha 1C$ in NRVMs. Representative images of NRVMs probed with rabbit anti- $\alpha 1C$ antibody/mouse anti-PC-1 antibody. Scale bar: 20 μ m. Values are mean \pm SEM analyzed by Wech's test, one-way ANOVA followed by Tukey's (n=3-5). * $P < 0.05$ vs. control.

Figure II. A, Engineering and genotyping of PC-1 KO mice. B, Baseline percent fractional shortening (%FS, left), LVEDD (center) and LVESD (right) in α -MHC cre and PC-1 KO mice. C, Echocardiographic time course data under basal conditions of α -MHC cre and PC-1 KO mice. D, $\alpha 1C$ Western blot under baseline conditions in α -MHC cre and PC-1 KO mice. Low- and high-exposure Western blots for $\alpha 1C$ are shown. E, *Pkd-1* mRNA levels depicted as *Pkd-1*/18S ratios. F, mRNA levels of *Pkd-2* (gene coding for PC-2) depicted as *Pkd-2*/18S ratios. G, PC-2 Western blot from α -MHC cre and PC-1 KO cardiac tissue in Sham- or TAC-operated mice. H, PC-2 protein levels shown in a bar graph from Western blot depicted in G. Values are mean \pm SEM analyzed by Student's unpaired *t*-test or Welch's test, one-way ANOVA followed by Tukey's test (n=5-8). * $P < 0.05$ vs. control.

Figure III. A, α 1C subunit protein detected by Western blot in Sham- or TAC-operated α -MHC cre and PC-1 KO mice. Low- and high-exposure Western blots for α 1C are shown B, β 2 Western blot from α -MHC cre and PC-1 KO cardiac tissue after Sham and TAC procedure. C, β 2 protein levels quantified from Western blot depicted in B. Values are mean \pm SEM analyzed by Welch's test, one-way ANOVA followed by Tukey's test (n=5). * P <0.05 vs. control.

Supplementary Tables

Supplementary Table 1

PCR primer pairs used to genotype PC-1 knockout mice.

Supplementary Table 2

PCR primer pairs used for quantitative RT-PCR.

ONLINE DATA SUPPLEMENT

Polycystin-1 is a Cardiomyocyte Mechanosensor that Governs L-type Ca²⁺ Channel Protein Stability

Zully Pedrozo, PhD^{1,2,7}; Alfredo Criollo, PhD^{3,7}; Pavan K. Battiprolu, PhD⁷;
Cyndi R. Morales, BS⁷; Ariel Contreras, PhD¹; Carolina Fernández, MSc¹;
Nan Jiang, MSc⁷; Xiang Luo, MD, PhD⁷; Michael J. Caplan, MD, PhD⁴;
Stefan Somlo, MD^{5,6}; Beverly A. Rothermel, PhD^{7,8}; Thomas G. Gillette, PhD⁷;
Sergio Lavandero, PhD^{1,2,7,#}; Joseph A. Hill, MD, PhD^{7,8,#}

¹Advanced Center for Chronic Diseases (ACCDiS) & Centro de Estudios Moleculares de la Célula (CMEC), Facultad de Medicina & Facultad de Ciencias Químicas y Farmacéuticas;
²Instituto de Ciencias Biomédicas, Facultad de Medicina; ³Instituto de Investigación en Ciencias Odontológicas, Facultad de Odontología, Universidad de Chile, Santiago, Chile;
Departments of ⁴Cellular and Molecular Physiology, ⁵Internal Medicine, and ⁶Genetics, Yale University School of Medicine, New Haven, CT; ⁷Division of Cardiology, Department of Internal Medicine, and the ⁸Department of Molecular Biology, University of Texas Southwestern Medical Center, Dallas, TX

Running title: PC-1-dependent mechanotransduction in heart

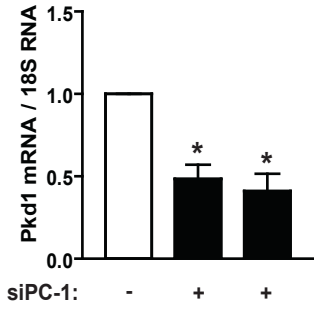
Correspondence to:

Joseph A. Hill, MD, PhD, Cardiology Division, Department of Internal Medicine
UT Southwestern Medical Center, 6000 Harry Hines Blvd, Dallas, TX 75390-8573
(joseph.hill@utsouthwestern.edu);

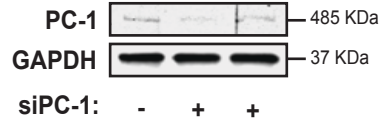
or Sergio Lavandero, PhD, Advanced Center for Chronic Diseases (ACCDiS),
Facultad de Ciencias Químicas & Facultad de Medicina,
Universidad de Chile, Olivos 1007, Santiago 8380492, Chile (slavander@uchile.cl).

Supplementary Figure I

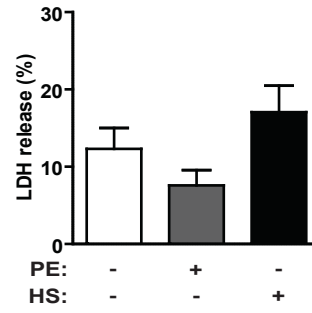
A



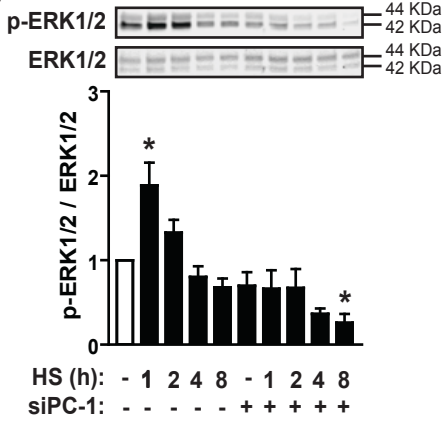
B



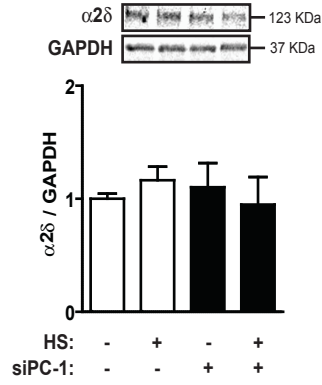
C



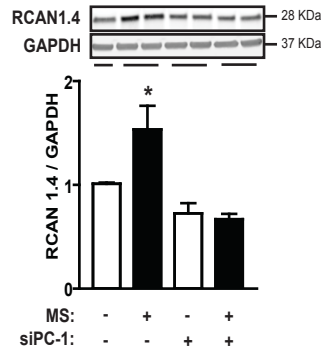
D



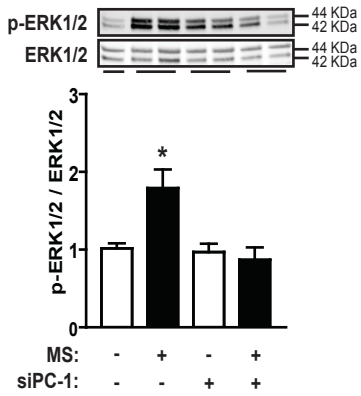
E



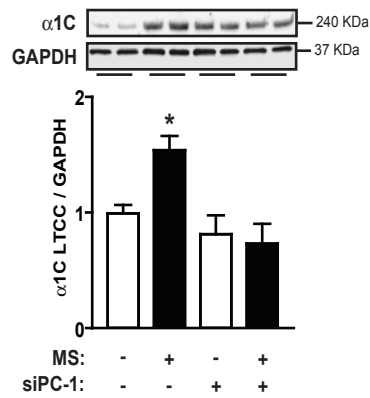
F



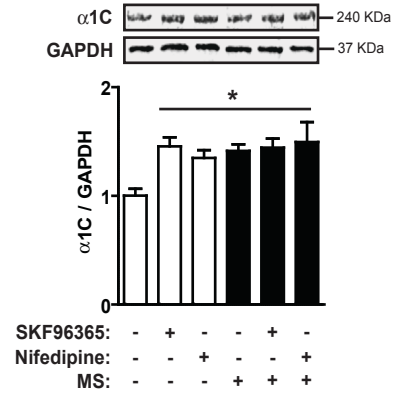
G



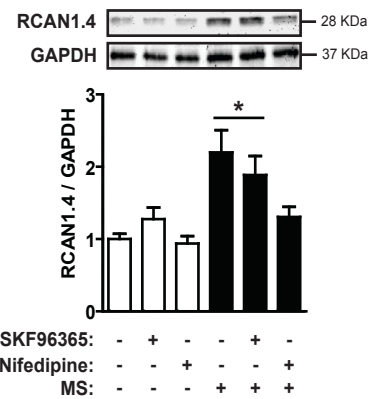
H



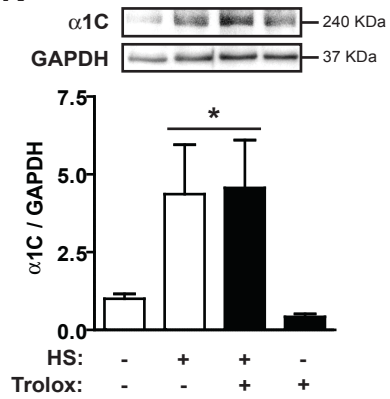
I



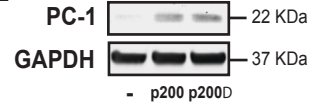
J



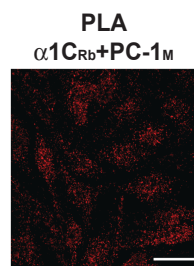
K



L

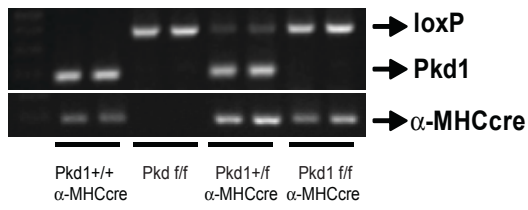


M

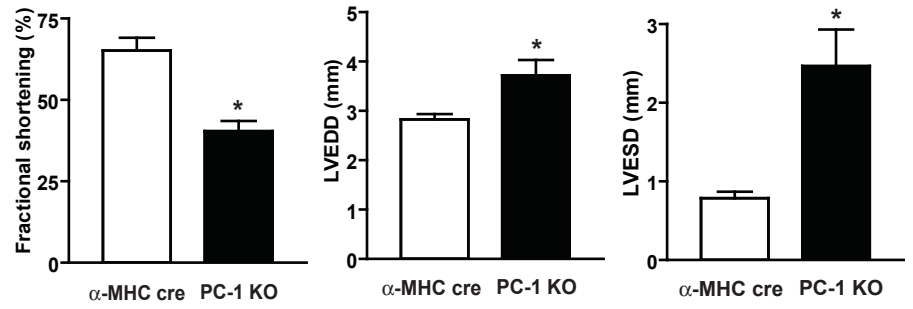


Supplementary Figure II.

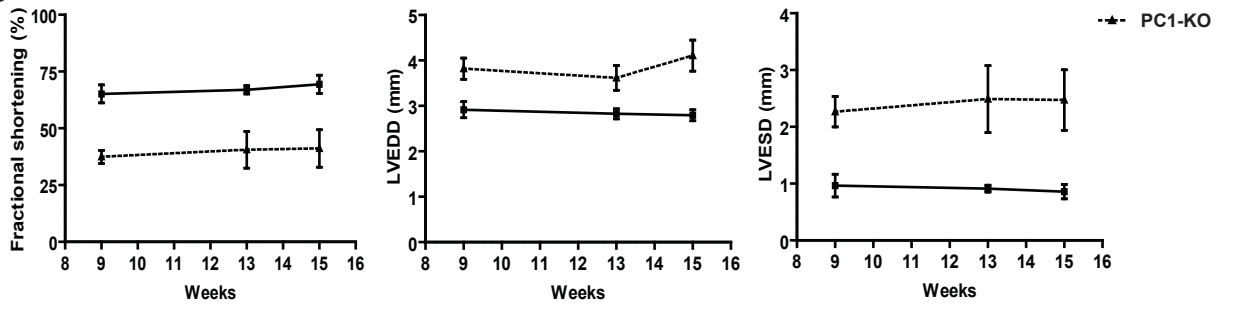
A



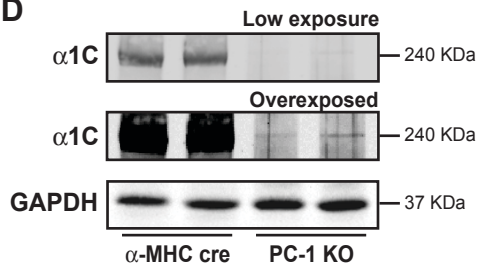
B



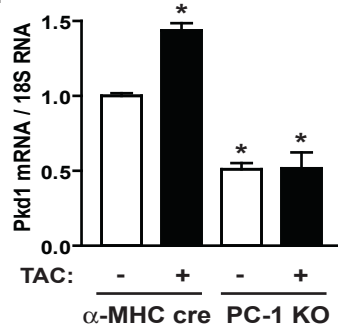
C



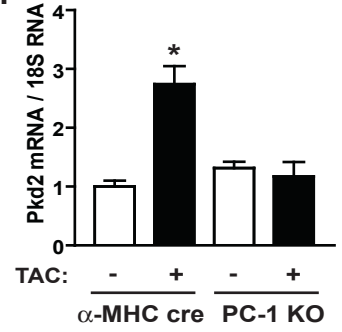
D



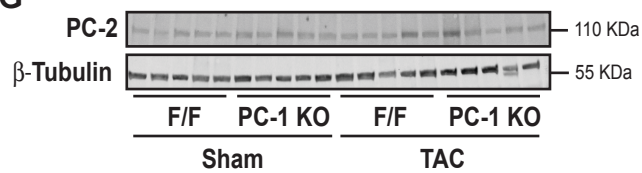
E



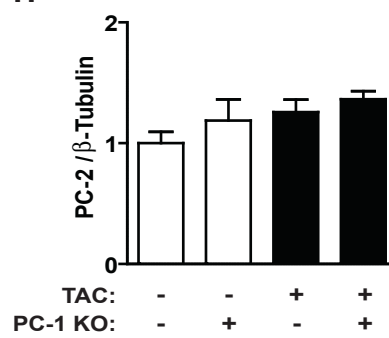
F



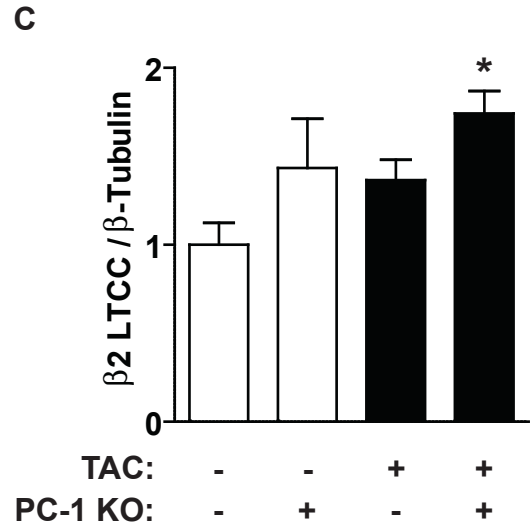
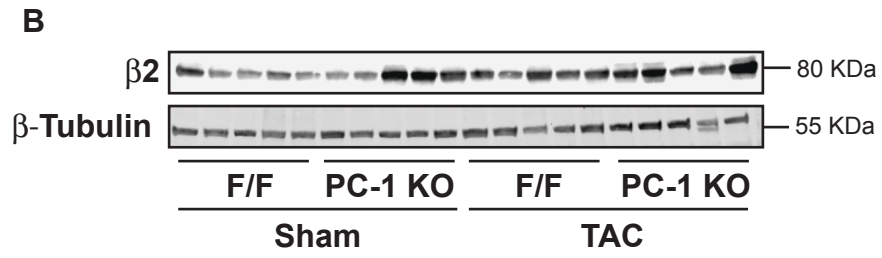
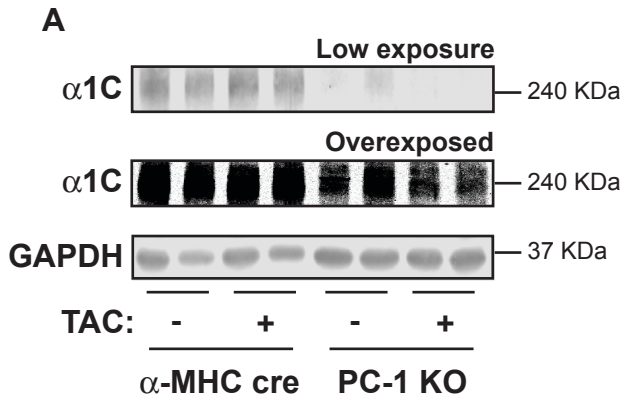
G



H



Supplementary Figure III.



Supplementary Table 1

Primer pairs used for Pkd-1 genotyping by PCR

Gene	Primer pair	
	Forward (5'-3')	Reverse (5'-3')
<i>Mouse</i>		
LOX	ccgctgtgtctcagtgccctg	caagagggcctttcttgctg
CRE	gatttcgaccagggttcgttc	gctaaccagcgttttcgttc

Supplementary Table 2

Primer pairs used for quantitative RT-PCR

Gene	Primer pair	
	Forward (5'-3')	Reverse (5'-3')
Mouse		
18S RNA	cggacaggattgacagattg	caaatcgctccaccaactaa
β -MHC	aagcagcagttggatgagcg	cctcgatgctgcctgaagc
ANF	cttctcctcgtcttggcct	ctgcttcctcagtctgctca
BNP	catggatctcctgaaggtgc	cctcaagagctgtctctgg
Pkd-1	gccatccagcacttcttagt	gagaagccgatccacacatc
Pkd-2	tgtgtggtcaggttattggcg	gccaggaagaaatcaaaggc
RCAN 1.4	cccgtgaaaaagcagaatgc	tccttgcatatgttctgaagaggg
α 1C	gttcttgattgctgcgaga	aagaaatgcagcaacagccg
Rat		
18S RNA	aaacggctaccacatccaag	cctccaatggatcctcgta
β -MHC	ctgactgaacagctgggctc	aactctggaggctcttcaact
RCAN 1.4	gacccgcgcgtgttc	tgatcatatgttctgaagaggattc
Pkd-1	gccatccagcacttcttagt	gaaaagccgatccacacgctc
Pkd-2	tgtgtggtcaggttattgggt	gccaggaagaaatcaaaggc
α 1C	agcaactccctcagacgtttg	gcttctcatgggacggtgat

Supplementary Figures

Figure I. A, *Pkd-1* mRNA levels from cardiomyocytes transfected with sequence-independent siRNA constructs targeting PC-1 (siPC-1) are depicted. B, PC-1 protein levels in cardiomyocytes transfected with 2 different, sequence-independent siRNAs. C, Cardiomyocyte death after exposure to phenylephrine (PE) or HS stimulation. Lactate dehydrogenase (LDH) activity was measured, and the results are shown as percent of LDH release in the culture medium. D, Representative Western blot for p-ERK1/2 and total ERK1/2 (above) and pERK1/2 / ERK1/2 ratio (below) in siPC-1 and controls cells. E, Representative Western blot for $\alpha 2\delta$ and quantification analysis in the bar graph. F, Western blots for RCAN1.4 and GAPDH (above) and quantification after mechanical stress (MS) stimulation (2 h). G, pERK1/2 and total ERK1/2 in control and siPC-1 cells stimulated with MS. H, $\alpha 1C$ protein levels after MS in control and siPC-1 cells. $\alpha 1C$ (I) and RCAN1.4 (J) representative Western blots after MS in presence of a SOCE inhibitor, SKF96365 or nifedipine and their corresponding quantifications. K, Representative Western blot for $\alpha 1C$ and densitometric analysis of cardiomyocytes stimulated with HS in presence of trolox. L, Western blot for PC-1 from NRVMs over-expressing PC-1 C-terminal peptide (p200) or the C-terminal peptide lacking the nuclear localization signal (p200 Δ). M, Duolink protein-protein interaction assay for PC-1 and $\alpha 1C$ in NRVMs. Representative images of NRVMs probed with rabbit anti- $\alpha 1C$ antibody/mouse anti-PC-1 antibody. Scale bar: 20 μ m. Values are mean \pm SEM analyzed by Wech's test, one-way ANOVA followed by Tukey's (n=3-5). * P <0.05 vs. control.

Figure II. A, Engineering and genotyping of PC-1 KO mice. B, Baseline percent fractional shortening (%FS, left), LVEDD (center) and LVESD (right) in α -MHC cre and PC-1 KO mice. C, Echocardiographic time course data under basal conditions of α -MHC cre and PC-1 KO mice. D, $\alpha 1C$ Western blot under baseline conditions in α -MHC cre and PC-1 KO mice. Low- and high-exposure Western blots for $\alpha 1C$ are shown. E, *Pkd-1* mRNA levels depicted as *Pkd-1*/18S ratios. F, mRNA levels of *Pkd-2* (gene coding for PC-2) depicted as *Pkd-2*/18S ratios. G, PC-2 Western blot from α -MHC cre and PC-1 KO cardiac tissue in Sham- or TAC-operated mice. H, PC-2 protein levels shown in a bar graph from Western blot depicted in G. Values are mean \pm SEM analyzed by Student's unpaired *t*-test or Welch's test, one-way ANOVA followed by Tukey's test (n=5-8). * P <0.05 vs. control.

Figure III. A, α 1C subunit protein detected by Western blot in Sham- or TAC-operated α -MHC cre and PC-1 KO mice. Low- and high-exposure Western blots for α 1C are shown B, β 2 Western blot from α -MHC cre and PC-1 KO cardiac tissue after Sham and TAC procedure. C, β 2 protein levels quantified from Western blot depicted in B. Values are mean \pm SEM analyzed by Welch's test, one-way ANOVA followed by Tukey's test (n=5). * P <0.05 vs. control.

Supplementary Tables

Supplementary Table 1

PCR primer pairs used to genotype PC-1 knockout mice.

Supplementary Table 2

PCR primer pairs used for quantitative RT-PCR.